

**COSIMA – HIGH RESOLUTION TIME-OF-FLIGHT SECONDARY ION  
MASS SPECTROMETER FOR THE ANALYSIS OF COMETARY DUST  
PARTICLES ONBOARD ROSETTA**

J. KISSEL<sup>1</sup>, K. ALTWEGG<sup>2</sup>, B. C. CLARK<sup>3</sup>, L. COLANGELI<sup>4</sup>, H. COTTIN<sup>5</sup>,  
S. CZEMPIEL<sup>6</sup>, J. EIBL<sup>6</sup>, C. ENGRAND<sup>7</sup>, H. M. FEHRINGER<sup>8</sup>, B. FEUERBACHER<sup>9</sup>,  
M. FOMENKOVA<sup>10</sup>, A. GLASMACHERS<sup>11</sup>, J. M. GREENBERG<sup>12</sup>, E. GRÜN<sup>13</sup>,  
G. HAERENDEL<sup>6</sup>, H. HENKEL<sup>14</sup>, M. HILCHENBACH<sup>1</sup>, H. VON HOERNER<sup>14</sup>,  
H. HÖFNER<sup>6</sup>, K. HORNING<sup>15</sup>, E. K. JESSBERGER<sup>16</sup>, A. KOCH<sup>14</sup>, H. KRÜGER<sup>1</sup>,  
Y. LANGEVIN<sup>17</sup>, P. PARIGGER<sup>6</sup>, F. RAULIN<sup>5</sup>, F. RÜDENAUER<sup>18</sup>, J. RYNÖ<sup>19</sup>,  
E. R. SCHMID<sup>20</sup>, R. SCHULZ<sup>8</sup>, J. SILÉN<sup>19</sup>, W. STEIGER<sup>21</sup>, T. STEPHAN<sup>16</sup>,  
L. THIRKELL<sup>22</sup>, R. THOMAS<sup>22</sup>, K. TORKAR<sup>23</sup>, N. G. UTTERBACK<sup>24</sup>,  
K. VARMUZA<sup>25</sup>, K. P. WANCZEK<sup>26</sup>, W. WERTHER<sup>20</sup> and H. ZSCHEEG<sup>27</sup>

<sup>1</sup>Max-Planck-Institut für Sonnensystemforschung, Max-Planck-Str. 2, 37191 Katlenburg-Lindau,  
Germany

<sup>2</sup>Physikalisches Institut, Universität Bern, Sidlerstr. 5, 3012 Bern, Switzerland

<sup>3</sup>Lockheed Martin Astronautics, Post Office Box 179, MS-B0560, Denver, CO 80201, USA

<sup>4</sup>Istituto Nazionale di Astrofisica – Osservatorio Astronomico di Capodimonte, Via Motariello 15,  
80131 Napoli, Italy

<sup>5</sup>LISA, Universites Paris 12 & Paris 7, Faculté des Sciences et Technologie, 61, Avenue du General  
de Gaulle, F-94010 Creteil Cedex, France

<sup>6</sup>Max-Planck-Institut für Extraterrestrische Physik, Giessenbachstrasse, 85740 Garching,  
Germany

<sup>7</sup>Centre de Spectrométrie Nucléaire et de Spectrométrie de Masse – CSNSM, Bat. 104, 91 405  
Orsay, France

<sup>8</sup>ESA – ESTEC, Postbus 299, 2200AG Noordwijk, The Netherlands

<sup>9</sup>Deutsches Zentrum für Luft- und Raumfahrt e.V. (DLR) in der Helmholtzgemeinschaft, Institut für  
Raumsimulation, Linder Höhe, D-51147 Köln, Germany

<sup>10</sup>Center for Astrophysics and Space Sciences, University of California San Diego, La Jolla,  
CA 92093-0424, USA

<sup>11</sup>Universität Wuppertal, FB-E, Lehrstuhl für Messtechnik, Rainer-Gruenter-Str. 21, 42119  
Wuppertal, Germany

<sup>12</sup>Raymond and Beverly Sackler Laboratory for Astrophysics, P.O. Box 9513, NL-2300 RA Leiden,  
The Netherlands, deceased Nov. 2001

<sup>13</sup>Max-Planck-Institut für Kernphysik, Saupfercheckweg 1, 69115 Heidelberg, Germany

<sup>14</sup>von Hoerner und Sulger GmbH, Schlossplatz 8, 68723 Schwetzingen, Germany

<sup>15</sup>Universität der Bundeswehr LRT-7, Werner Heisenberg Weg 39, 85577 Neubiberg, Germany

<sup>16</sup>Institut für Planetologie, Wilhelm-Klemm-Str. 10, 48149 Münster, Germany

<sup>17</sup>Institut d'Astrophysique, Batiment 121, Faculté des Sciences d'Orsay, 91405 Orsay, France

<sup>18</sup>Institut f. Physik, Forschungszentrum Seibersdorf, 2444 Seibersdorf, Austria

<sup>19</sup>Finnish Meteorological Institute, Department of Geophysics, rik Palménin aukio 1, FI-00560  
Helsinki, Finland

<sup>20</sup>Department of Analytical and Food Chemistry, University of Vienna, Währingerstrasse 38,  
A-1090 Vienna, Austria

<sup>21</sup>ARC Seibersdorf Research GmbH Business Field Aerospace Technology, 2444 Seibersdorf,  
Austria

<sup>22</sup>Laboratoire de Phys. & Chim. de L'Environnement, 3 Av. de la Recherche Scientifique, 45071  
Orléans, France

J. KISSEL ET AL.

<sup>23</sup>*Institut für Weltraumforschung, Österreichische Akademie der Wissenschaften, Schmiedlstrasse 6,  
8042 Graz, Austria*

<sup>24</sup>*Consultant, 93105 Sta. Barbara, CA, USA, deceased Nov. 2003*

<sup>25</sup>*Vienna University of Technology, Institute of Chemical Engineering, Getreidemarkt 9/166, A-1060  
Vienna, Austria*

<sup>26</sup>*Institut für Anorganische und Physikalische Chemie, Universität Bremen, Haferwende 12, 28357  
Bremen, Germany*

<sup>27</sup>*Abbott Laboratories Vascular Devices Ltd., Amphauptstrasse, 8222 Beringen, Switzerland  
(\*Author for correspondence: E-mail: cometkissel@arcor.de)*

(Received 22 March 2006; Accepted in final form 11 October 2006)

**Abstract.** The ESA mission Rosetta, launched on March 2nd, 2004, carries an instrument suite to the comet 67P/Churyumov-Gerasimenko. The COmetary Secondary Ion Mass Analyzer – COSIMA – is one of three cometary dust analyzing instruments onboard Rosetta. COSIMA is based on the analytic measurement method of secondary ion mass spectrometry (SIMS). The experiment's goal is in-situ analysis of the elemental composition (and isotopic composition of key elements) of cometary grains. The chemical characterization will include the main organic components, present homologous and functional groups, as well as the mineralogical and petrographical classification of the inorganic phases. All this analysis is closely related to the chemistry and history of the early solar system. COSIMA covers a mass range from 1 to 3500 amu with a mass resolution  $m/\Delta m @ 50\%$  of 2000 at mass 100 amu. Cometary dust is collected on special, metal covered, targets, which are handled by a target manipulation unit. Once exposed to the cometary dust environment, the collected dust grains are located on the target by a microscopic camera. A pulsed primary indium ion beam (among other entities) releases secondary ions from the dust grains. These ions, either positive or negative, are selected and accelerated by electrical fields and travel a well-defined distance through a drift tube and an ion reflector. A microsphere plate with dedicated amplifier is used to detect the ions. The arrival times of the ions are digitized, and the mass spectra of the secondary ions are calculated from these time-of-flight spectra. Through the instrument commissioning, COSIMA took the very first SIMS spectra of the targets in space. COSIMA will be the first instrument applying the SIMS technique in-situ to cometary grain analysis as Rosetta approaches the comet 67P/Churyumov-Gerasimenko, after a long journey of 10 years, in 2014.

## 1. Introduction

The *in situ* chemical analysis of solids in space is among the tasks that are technically most difficult. There are two main reasons for that: With a few exceptions, solids in space are not abundant, and, secondly, it is not easy to remove small samples from the solid into the vacuum for the analysis in a mass spectrometer.

For COSIMA, the objects of interest are cometary dust particles, which are abundant, indeed, in the neighborhood of the comet nucleus. It remains, however, to collect and bring the particles to the entrance of the spectrometer.

Most mass spectrometers need the parts of the sample to be analyzed, to carry an electric charge. The process of removing an ion from the specimen is then the critical feature of the method to be chosen.

The only mass spectrometric data on cometary dust particles available to date come from the dust impact mass spectrometers PIA, PUMA, and CIDA on the GIOTTO, VEGA, and Stardust spacecrafts, respectively. (Far more and more detailed mass spectra of IDPs of supposed cometary origin are available from laboratory measurements, and soon there will be results from the cometary dust particles retrieved from Stardust.) While other, remote, or indirect methods allow measurements of collective properties of the cometary dust, the mass spectrometers allowed the analysis of individual particles (cf. Kissel *et al.*, 1986a, b). Since then, we know unambiguously that each particle is an intimate mixture of a mineral component and simple as well as complex organic molecules. Since the impact velocity was large ( $>60$  km/s), mostly atomic ions were formed and analyzed in the Halley case. In a first attempt, however, Kissel and Krueger (1987) found evidence for the chemical nature of the organic cometary material. It is clear that not only a few well known molecules constitute the cometary organics, but rather several chemical classes, with each being represented by a large number of individual substances. Indeed, it seems possible that all stable molecules compatible with the chemical environment are formed.

COSIMA therefore needed to be based on a method, which is readily available in laboratory, and which allows for tracing the ion directly to the molecular and structural form in which it was present in the solid. Since the size distribution of the dust particles is known (cf. Mazets *et al.*, 1987; McDonnell *et al.*, 1989), a reasonable ionizing beam focus should be achieved under the limitations of space instrumentation. Even though the method would be destructive, its sensitivity should be high enough to allow several analyses at different depths for one individual  $\sim 20$   $\mu\text{m}$  particle.

To satisfy all these requirements, we choose the method of Secondary Ion Mass Spectrometry (SIMS). A fast primary ion, in this case  $^{115}\text{In}^+$  at 8 keV, impacts the sample and releases by desorption atoms and molecules of the sample, of which typically 0.1 to 10% are ionized, the so-called secondary ions. For sensitivity reasons, the analysis of a rather large mass range should be achieved simultaneously, which in turn leads to the type of a time-of-flight mass spectrometer. The mass resolution must be high enough to resolve isobaric ions, at least atomic from molecular ions. The mass range should at least cover 3500 amu. In total, the COSIMA instrument has the following main functional hardware elements:

- dust collector and target manipulator,
- COSISCOPE, a microscope for target inspection
- primary ion source, and
- mass spectrometer including the ion extraction optics and the ion detector.

Of course, for autonomous operation, the entire instrument is under microprocessor based software control.

It should be mentioned at this point that COSIMA did profit from but is not identical to the earlier development of the CoMA instrument for the NASA mission CRAF (Zscheeg, 1992), which was canceled in 1992.

The entire development of COSIMA was challenged by the complexity of especially the organic cometary material, which has to be expected. This has focused the goal of COSIMA on the identification of chemical classes and functional groups rather than the identification of individual substances. Consequently the system must have the capability to use the methods of chemometrics to compress the raw data on board, which helps to reduce the data volume without losing any of the chemical information.

There is also another important aspect for COSIMA, which comes from the rather long time the spacecraft travels from launch in 2004 until the core of the measurements takes place in 2014: Quite a large number of relevant results will be obtained from laboratory measurements with TOF-SIMS, potentially by the COSIMA team or in the published literature. In addition, NASA in its DISCOVERY program has several comet missions, which are expected to produce new, relevant data, before COSIMA enters its main analysis phase. Even if most of the flexibility is with the software involved, it is the hardware, which has to provide the resources necessary. Looking back at the fast development in the computer sector over the last ten years, this alone is a demanding task, even without the complexity of an up-to-date analysis instrument.

The overall parameters and resources describing COSIMA are:

- Atomic mass range 1 . . . 3500 amu
- Rel. atomic mass resolution  $m/\Delta m$  (at  $m = 100$  amu)  $>2000$  at 50% peak width
- Indium ion pulse duration  $<3$  ns
- Indium ion energy 8 keV
- Ion beam width about 50  $\mu\text{m}$  FWHM
- Telemetry rate about 500 bit/sec
- Mass 19.8 kg
- Power consumption from 28 V DC 20.4 W

## 2. Functional Description

COSIMA is a time-of-flight secondary ion mass spectrometer. Like all such instruments, primary ions generate secondary ions from a target, which they hit. Those secondary ions are then accelerated to the same, constant kinetic energy, and their flight time to the ion detector is measured. This flight time follows the equation:

$$\text{time-of-flight} = a \times (\text{mass}/\text{abs}(q))^{0.5} + b; \quad (1)$$

with  $a$  is an instrumental constant depending on the length of the flight path and the electrical voltages applied, for COSIMA it is about  $3.1 \mu\text{s}/(\text{mass})^{0.5}$ ;  $b$  is a constant for the offset of the time measurement; mass is the ion mass in amu;  $q$  is the ion charge state, in most cases =  $-1$  or  $+1$ .

The schematic view of the COSIMA functional blocks is shown in Figure 1. COSIMA works pretty much like a laboratory instrument, with a somewhat reduced performance due to the limitations for a space instrument, but remotely operated in a ‘distant lab’. The limitations come first of all from the mass and power available, but more pronounced from the limited capacity of data transfer to and from the instrument, combined with a reaction time (round trip time delay) of 32 minutes during the main operation time.

Consequently the individual steps for the analysis of a dust particle are:

- (1) exposure of a collection substrate for a predetermined time
- (2) optical search of the substrate for dust particles by the camera system COSIS-COPE
- (3a) moving a dust particle in front of the spectrometer
- (3b) either first clean the particle and surrounding by sputtering or
- (3c) start the particle characterization
- (4) decide if a detailed analysis is promising

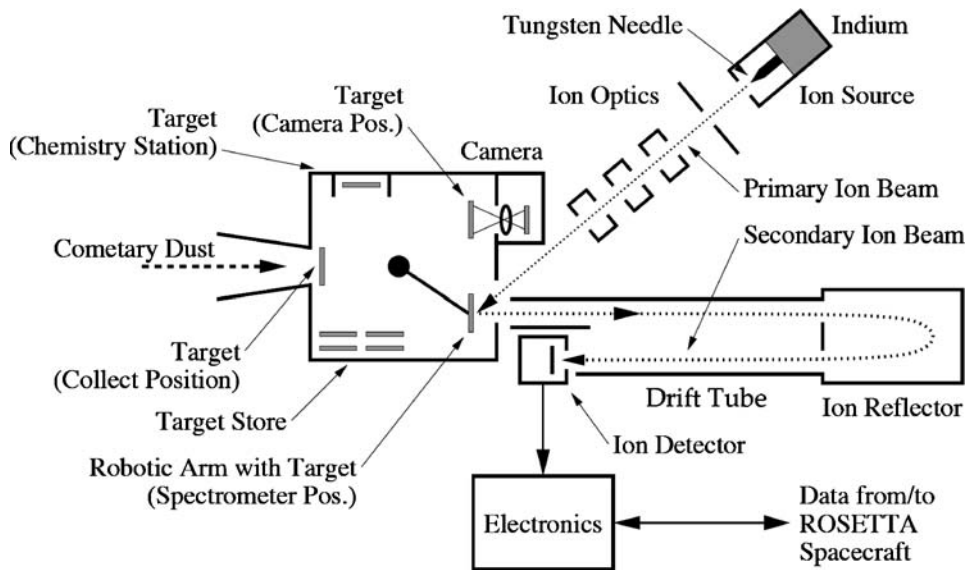
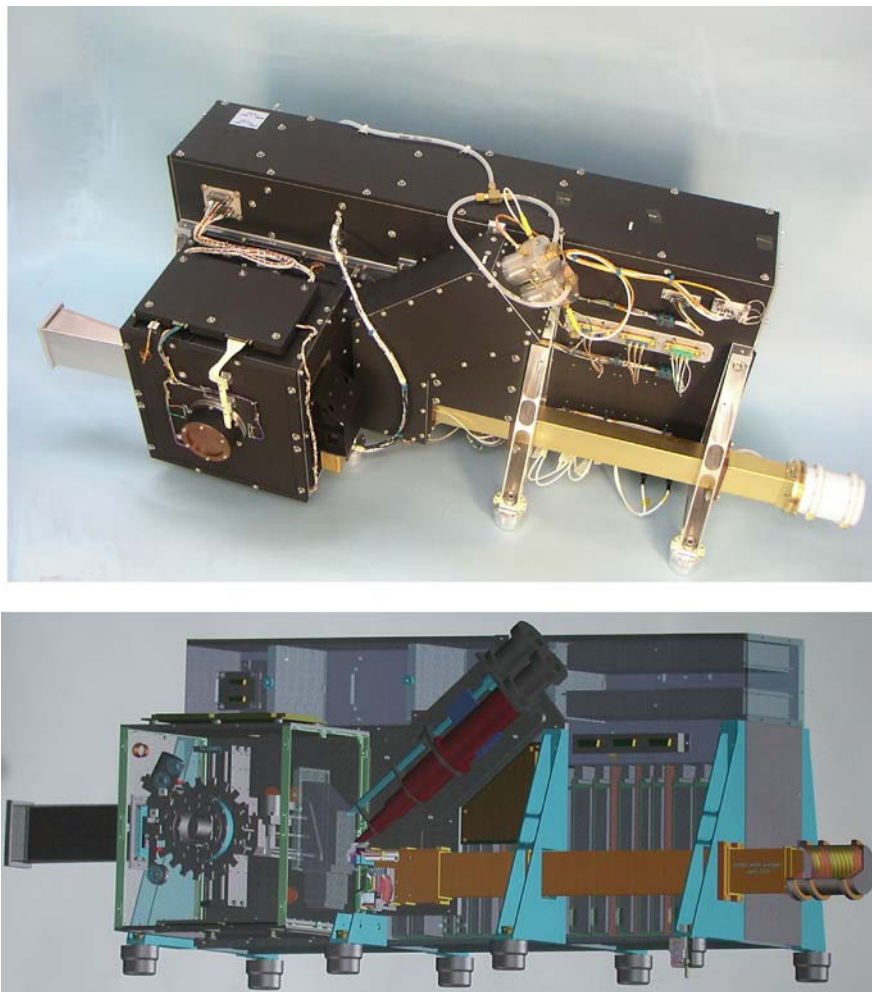


Figure 1. Schematic view of the COSIMA instrument: (1) Dust is collected on metal targets, (2) Positions of dust grains are determined by microscopic camera, (3) A pulsed primary ion beam sputters and partially ionizes the cometary material, (4) Secondary ions are accelerated by an electric field and travel through the time-of-flight section – a drift tube with an ion reflector, (5) Mass spectra data are extracted from the resulting time-of-flight spectra.

- (5) if so, do a detailed analysis in both, the positive and negative, ion modes
- (6) perform onboard chemistry
- (7) do another detailed analysis in both, the positive and the negative, ion modes
- (8) move to the next particle

In favor of clarity, the instrument's function is described in terms of the analysis steps above, while the more elaborate description of the subunits follows. See Figures 1 and 2 to locate the functional elements. As described in more detail below, COSIMA has dedicated surfaces for the collection of cometary dust particles. These



*Figure 2.* COSIMA instrument (flight model and 3D drawing). The COSIMA flight model consists of dust funnel, target manipulation unit (TMU), primary indium ion sources (PIS) with the primary ion beam subsystem (PIBS), the high-resolution mass spectrometer with ion detector, all mounted onto the COSIMA electronic box.

may impact with their release speed of the order of 100 m/s. Since SIMS is a very sensitive method, the collection surfaces need to be a material, which does not interfere with the type of materials expected in the dust. This excluded any kind of organic material. A study performed by Krueger (1988) identified metal blacks as suitable materials from the structural, and silver, palladium, gold, or platinum from the material properties point of view. The choice has turned out to be very sensible, as these blacks are also efficient pumps for contaminants unavoidable for a space instrument. Since the cometary particles can have a wide range of speeds depending on their size and on the gas activity of the nucleus, each unit of targets has three  $1 \times 1 \text{ cm}^2$  collection areas (substrates) and a separate  $0.3 \times 3 \text{ cm}^2$  strip as an unexposed reference area. Always an entire target assembly (see Figure 3) is exposed at a time.

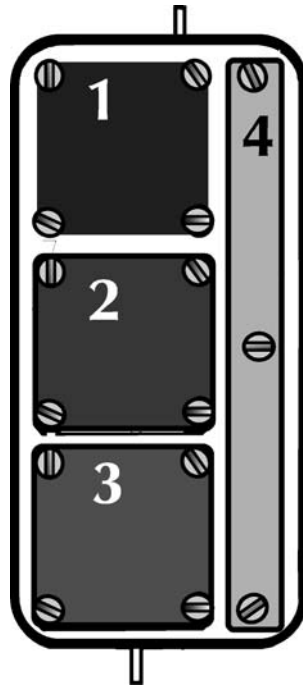


*Figure 3.* COSIMA Target Assembly. Three individually prepared and selected target plates for dust collection and a reference strip, which will not be exposed to dust make up a target assembly. Each target is numbered individually, and the coordinate system coincides with the S/C coordinate system in the COSISCOPE, ANALYZE, and CLEAN positions (see text). For each collection substrate the coordinate system starts at the lower left corner. Laser generated bright spots of  $50 \mu\text{m}$  diameter (not shown) make it possible for COSISCOPE to identify the individual substrate, to define the position of the substrate in its field-of-view, and to determine of the relative positions of collected dust in the substrate reference frame. Specific dust grains can then be analyzed by moving them under spectrometer's primary beam using the TMU.

Manipulation of the target units is achieved with the Target Manipulator Unit (TMU), which was designed and added at a late state when a contributed system by our Italian partners did not materialize. As built by MPE and Cemec (Schwab, 1998) it is a semi-autonomous system, which provides access to the positions 'COLLECT', 'STORE', 'COSISCOPE', 'CLEAN', 'ANALYZE', and 'CHEMISTRY' upon simple (internal) commands.

The first inspection of the sample is done by COSISCOPE, a COSIMA internal camera. One of the 3 collection substrates is checked at a time. Light beams from two sets of LEDs left and right of the sample illuminate it. The images are checked for features like, e.g., shadows and interpreted as sites, the coordinates of which are transferred to the main instrument.

The next step is the decision if the target, or a part of it, needs cleaning by ion-sputtering. If so, it is moved in front of a DC ion beam at the 'CLEAN' position, else, it will be presented to the mass spectrometer. The primary ion source (PIBS) has a separate beam for cleaning, providing 10–100  $\mu\text{A}$  on a 100  $\mu\text{m}$  diameter spot equivalent to removing some 100 monolayers per second. The next step is to analyze a site, i.e., to take a mass spectrum. The target is put in front of the extraction lens of the spectrometer, with the selected site within 100  $\mu\text{m}$  of the lens' center. Operational values are taken from the initial adjustment of the primary ion source. Trains of ion packages of 3 ns width at a rate of 1 kHz release secondary ions into the spectrometer. Its second order focusing design provides an inherent mass resolution of  $m/\Delta m @ 50\%$  peak height above 3000 (i.e., with 0-time spread of the primary beam). A typical primary ion package has 500 ions and releases 1 to 10 non-hydrogen secondary ions, depending on the material irradiated.

All secondary ions of the appropriate polarity are picked up by the electric field in front of the ion extraction lens. This field of about 1 kV/mm minimizes initial time-of-flight differences due to the acceleration process, which cannot be compensated later. The lens field also guides the ions into the time-of-flight section of the instrument reducing their drift energy to nominally 1 keV and focuses their arrival location on the detector into a 15 mm diameter area. As the ions travel down the drift tube, they pass the secondary deflection plates, which are needed to reposition the secondary ion package, should the analysis site be off center. It is also used to compensate the small changes in ion trajectories between the positive and negative secondary ions modes. At the end of the drift tube the ions enter the ion reflector, the device, which improves the intrinsic mass resolution of the spectrometer part by more than a factor of 100 (Mamyrin *et al.*, 1973). State-of-the-art would be a grid-less reflector (which we have studied) but which is very sensitive to the position of the ion entry and thereby on the perfect function of the secondary deflection plates. The actual design we have chosen uses several grids separating the drift section, the retarding section, and the reflecting section. As the ions enter under a small angle of  $1^\circ$ , they exit at a slightly different location but again into the same physical drift tube. At the end of this tube the ions hit the ion detector. The position and the orientation of the detector were carefully chosen,

as both are part of the system, which determines the mass resolution of COSIMA. Since we expect some of the organic ions to have high masses (well above 350 amu) the detector can be biased for a post-acceleration of the secondary ions by almost 9 kV (with the appropriate polarity for the respective ion type). The active element is a microsphere plate, which for its thickness of 1.4 mm provides a gain value well above  $10^7$ . In order to decouple the signal from its high electrical potential (up to 14 kV in the case of negative secondary ions), the microsphere output is directed to an anode, which is one side of a capacitor, while the other side is connected to the input of a pulse amplifier. All arrival times and shot numbers are stored at 2 ns resolution. The differences between the modes for positive or negative secondary ions are reflected in the respective operational voltages. Besides the reversal of polarity, minor adjustments need to be applied to the voltages for the deflection plates of both, the primary beam and the secondary ion path. The safe switch-over from one ion type to the other will take a couple of minutes to allow the high voltages to decay, before the grounding of the power supplies is switched.

A total of 1000 (adjustable) secondary ion arrival times are accumulated into the time-bins of a time-of-flight spectrum. While the measurement is continued, a peak list is created from this set of data, which is then further pre-evaluated using mathematical tools like classifiers developed for chemometrics (see below). This procedure yields criteria, which characterize the site under analysis. Should these criteria suggest a high similarity with another site already analyzed, then this fact is documented and the instrument proceeds to the next site on the list. The degree of autonomy is assigned to the instrument by telecommand from ground. This type of operation is necessary, as the reaction time for normal operational procedures via ground loop may well be of the order of a week, while the efficient use of the resources of the instrument rather requires a full-time operation.

The individual, functional elements of COSIMA mentioned in this chapter are described in more detail below.

### **3. The Functional Elements of COSIMA**

#### **3.1. THE MECHANICAL AND ELECTRICAL LAYOUT**

The properties of a time-of-flight mass spectrometer are determined by its mechanical elements and their respective electrical potentials. The mechanical centerpiece is the target substrate, upon which the cometary dust particles are collected. For the analysis, their surface has to point towards the spectrometer. Dust cannot be collected in the same position even with the same orientation: the targets have to be mechanically moved. In addition, different target materials and/or surface configurations are needed. Therefore several target units are made available. These few requirements together necessitate that the target surfaces be best kept at 0 V instrument potential, which then is the potential from which the secondary ions start.

To produce these secondary ions, the primary ion source must point its beam to a spot in front of the secondary ion extraction lens. In order to minimize interference between the beams, the primary ion source is usually inclined. An angle of  $45^\circ \pm 15^\circ$  in elevation is usually acceptable. In azimuth the angle is free to be chosen. Larger values lead to increasingly oblique impacts of the primary ions, increasing not only the spot size, but also the ion arrival time distribution and hence, the secondary ion emission time distribution. Smaller angles make the interface more complicated and increase the length necessary to assemble all the elements of the primary beam system. For COSIMA, an angle of  $50^\circ$  above the target plane (i.e.,  $40^\circ$  from the target normal) was chosen.

The extraction lens is usually arranged co-axially with the center target normal. For COSIMA, it is tilted by  $1^\circ$  towards the ion detector to provide the necessary offset for the secondary ions to reach the ion detector (rather than to fly back to the target). The rest of the mechanical elements of the mass spectrometer are the first (or inbound) drift tube, the reflector, the second (or outbound) drift tube, and the ion detector. For COSIMA these elements are essentially placed again co-axially with the center target normal with the following modification: the detector is moved away from the target center to the degree that it can be placed entirely besides the target. The reflector is placed such that its center axis lies in the plane of the target normal and the detector normal at mid-angle, as shown schematically in Figure 1. The inbound and outbound drift tubes are combined into one, which is wide enough to cover the natural expansion of the secondary ion beam as well as the displacement between the target and the ion detector.

The electrical layout is straightforward: The target is at 0 V instrument potential, and by the secondary ion extraction lens, the ions are accelerated to the drift potential of  $-/+1$  kV for positive or negative ions, respectively. The reflector, first introduced by Mamyrin *et al.*, (1973), has essentially the task to compensate for differences in total flight time, which occur as the ions start with different initial energies. Ions with higher kinetic energy penetrate deeper into the reflecting field and use more time to return from it. The best compensation occurs, when the ions spend about the same time in the reflector as they spend in the drift tubes. As the reflector is mechanically much shorter, it also helps to reduce the overall instrument length. For COSIMA, we chose a two stage reflector with a first retarding section, where the ions loose about 80% of their energy, and a second, reflecting section, where their direction of motion is reversed. The end of this section is formed by a grid, which should help to reduce background signals, caused by, e.g., neutral decay products from the secondary ions.

### 3.2. THE TARGET MANIPULATOR UNIT

When COSIMA was proposed for ROSETTA, it included a dust collector subsystem, the design of which was inherited from the CoMA/CRAF instrument. Later,

the idea of a dedicated COSIMA target manipulation was followed up, relying on a higher degree of integration into COSIMA’s mechanical and electrical subunits. This opened the chance for a redesign (Schwab 1998).

As will be described below, three individual target substrates (designed to collect dust) and a reference strip (not to be exposed to dust) are screwed down on a target holder and together make up the target assembly, which is to be manipulated. The new feature is that the target assemblies can now be moved individually, which includes the fact that they are released, once they are at their destination. This is achieved by the use of a grasping device working like a pair of tongs (see Figure 4). They are open when approaching the target assembly, and only, when they are tight

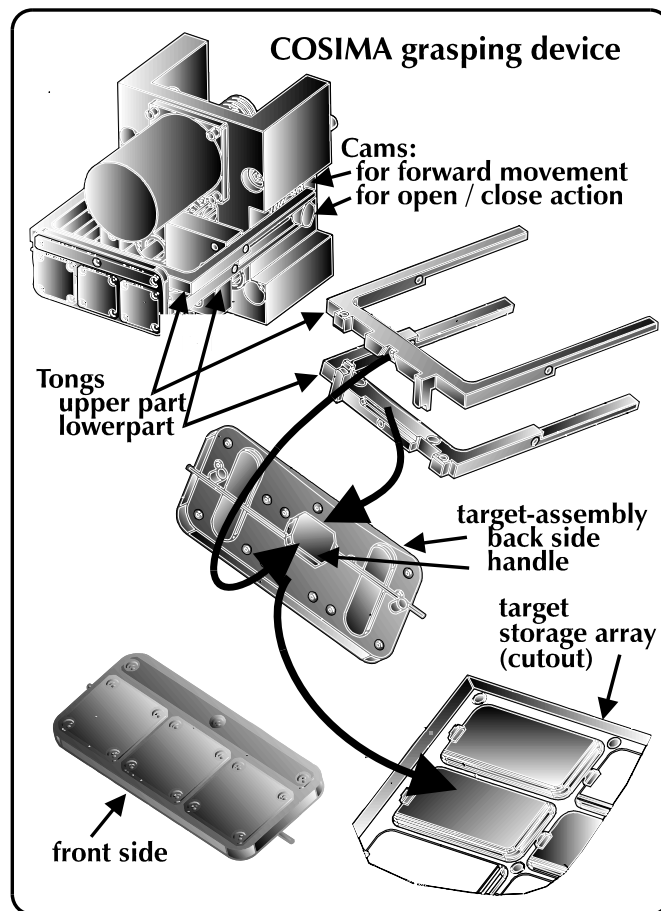


Figure 4. COSIMA Grasping Device. The COSIMA grasping device handles the internal transport of targets between individual stations. A single motor actuates the forward movement, the pick-up, deposit action and withdrawal with the help of two customized cams, controlling and synchronizing the movement. The device is mounted on an x-y-table (not shown).

enough not to let the object loose, they push on a spring, which latches the target assembly to the momentary position. When the object is firmly held, it is removed far enough to allow lateral and rotational motion. The motion in the forward and backward direction is actuated by a stepper motor, the opening and closing of the tongs is synchronized by a pair of cams. These cams have a specially designed shape. For one cam, the radial distance to its axis directly corresponds to the forward movement of the tongs. The other cam is fixed to the first, and its shape directly controls the opening action. The entire cycle of forward movement, opening/closing the tongs, and moving back takes less than one rotation of the axis. The sense of the axis rotation determines if a target assembly is picked up or deposited.

The housing of the Target Manipulator Unit is a rectangular box. In the center of the sides 1 and 6 (numbered as the sides of a dice) is a rotation axis, which carries an x-y table with the grasping device on top. In this way, targets can be reached on all remaining surfaces 2–5. These have the exact distance for the grasping device to properly pick up and place target assemblies. Let surface ‘2’ be at the ‘forward’ end of COSIMA, where the position for the dust collection is, then the COSISCOPE, ANALYZE, and CLEAN positions are on surface ‘5’. Surface ‘3’ is on the bottom of the box and carries the target storage area, where 24 target assemblies are stored in 6 rows of 4 positions each. This location is facing a radiator on the spacecraft skin, which allows the targets to be kept below about 30 °C even if the spacecraft interior is at 50 °C. On surface ‘4’ is the chemistry station and on surface ‘1’ is a docking structure, to which the grasping device will be locked during launch.

### 3.2.1. *Collection Substrates*

To meet its scientific requirements, COSIMA needs cometary dust particles for the analysis. Such dust particles are emitted by the cometary nucleus when its activity sets on under the influence of the solar heat input by radiation. The activity level of the comet depends on its position in the orbit, especially on the distance from the sun. Dust particles in the size range of 10  $\mu\text{m}$  and above are expected to reach speeds of up to a few 100 m/s. To collect these particles, appropriate surfaces were designed. Within COSIMA the dust particles are trapped in metal black layers of a few 10  $\mu\text{m}$  thickness, placed on top of square shaped 1×1 cm<sup>2</sup> metal plates of 0.5 mm thickness. Most of the substrates are made of gold and silver blacks, formed by evaporation of Au or Ag in a low pressure argon atmosphere. The Ar-atoms trigger the formation of nanometer-sized condensate particles, which deposit on the cold surface of the plates. They form a layer of loosely packed particles, sticking together and to the substrate by adhesive forces. The layer is thermally stable up to about 200°C. At higher temperatures, it collapses in a “sintering-like” process to a more dense structure, which loses its dark blackness to grey, but not its dust collection capability. The final configuration of this variant will be a multilayer structure, consisting of two “sintered” layers and one deep black on top of it, thus combining mechanical stability and blackness. A SEM image of an Ag-black layer is shown in Figure 5. Tests with SIMS showed that such blacks are not only optically

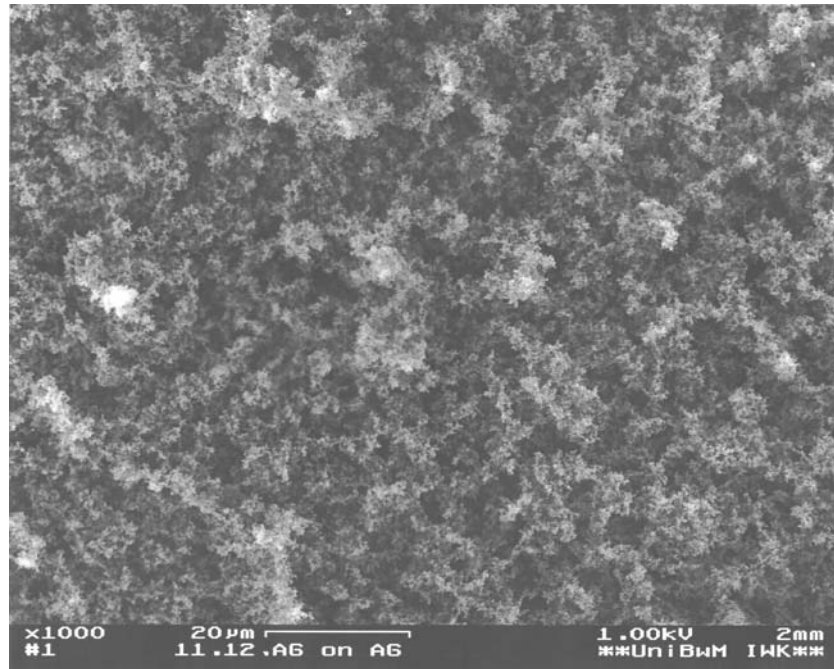


*Figure 5.* SEM image of an Ag-black layer. The COSIMA dust collection substrates are very evenly layers of Ag-black, which are soft enough to decelerate cometary dust and to keep it on their surface.

black, but also in the ion image, since the loose structure allows fewer secondary ions to reach the spectrometer.

Besides vapor deposited Au and Ag layers, some of the collection substrates are made from Pt and a few from Pd. Those types are manufactured by HERAEUS Noble Metal Techniques GmbH in Hanau/Germany, meeting the special needs for COSIMA. There are two types of platinum black substrates. One is made by anodic electro-deposition with subsequent sintering, which is needed for good mechanical contact to the backing as well as inner cohesion. As a result of the sintering process, the albedo of that substrate is not very low. The other is made by a proprietary method (patent pending) and produces a very black substrate with good mechanical connection to the backing. In either case, no residues from the production process were found by TOF-SIMS analysis. This was established after a long development procedure. Another substrate was palladium black on palladium foils, the production of which is difficult, due to the ultrahigh hydrogen pressure built up within the palladium bulk by the electro-deposition process. The mechanical properties of those three blacks differ from each other. Moreover, they are all harder than the vapor deposited blacks from gold or silver. A SEM picture of such a black is shown in Figure 6. It has a cauliflower-like structure and is mechanically much more firm

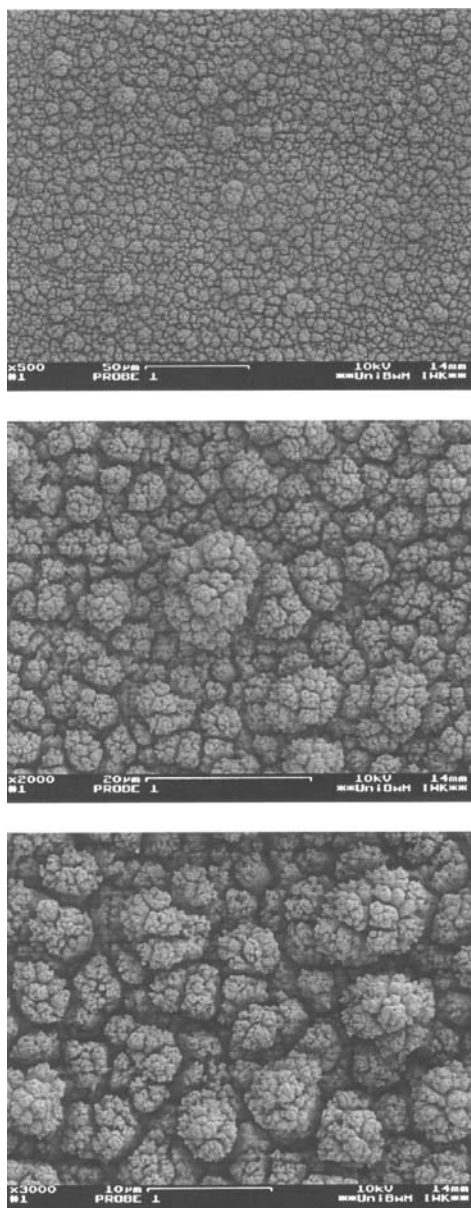


*Figure 6.* SEM picture of a liquid-deposited black. These collection substrates are thicker than those made by vapor deposition, and can be made from different materials. They usually show a 'cauliflower' like surface structure, in which smaller grains could be trapped and escape analysis.

than the vapor deposited blacks, which are thought to be used to trap very soft dust particles.

All blacks are marked directly after production at defined positions by pulse-laser generated test spots of about 50  $\mu\text{m}$  size. These spots can be recognized optically

(COSISCOPE) and by SIMS as well, thus defining a precise local coordinate system for common reference. Moreover, they serve for in-flight tests, such as adjustment of the ion beam's focusing.

Collection efficiency was tested by a gasdynamic accelerator for dust particles. It consists of a small tube (2 mm diameter) filled with argon or xenon as well as a very small amount of dust. The fast opening of a valve to an attached vacuum vessel generates a rarefaction wave, which accelerates the gas and the dust to the vessel and to the target. Velocities were checked by Laser Doppler Anemometry to be in the 50–150 m/s range. A SIMS image of some SiO<sub>2</sub> particles, sitting on a vapor deposited gold black are shown in Figure 7 (the picture shows the spatial distribution of the Si-line).

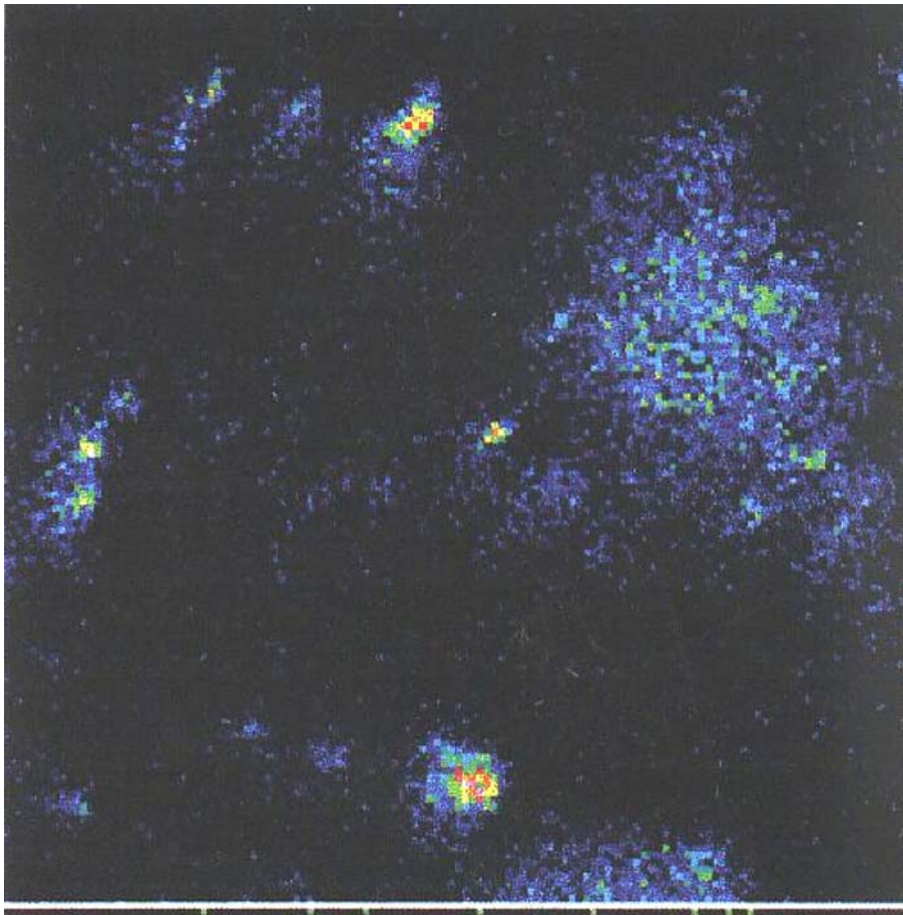


*Figure 7.* SIMS image of some SiO<sub>2</sub> particles, Si<sup>+</sup> spatial distribution. When particles are collected on the substrates, they can be found by COSIMA's primary ion source looking for indicative mass lines. Here is an example for silicate particles, detected by the Si<sup>+</sup>-intensity-distribution.

### 3.2.2. *The Chemistry Station*

A 'chemistry station' is located opposite to the storage system. It is a heating place for one target assembly. When TOF-SIMS mass spectra have been taken from cometary dust collected upon a target assembly, there may be some open questions concerning the chemistry. One concerns the distribution of molecular weights of certain organic species of the dust. Heating the specimen causes the smaller molecules to evaporate faster according to their specific heat of evaporation. This depends not only on the molecular weights but also on the distribution of polar groups in the molecules (Krueger *et al.*, 1991). Another question is, whether oxygen found in the organic material is present as OH-groups (as in sugars), which would eliminate water by heating. To provide clues to answering those questions, the samples need to be heated to about 100–140 °C.

### 3.3. COSISCOPE

During the early close-encounter-phase of the mission, the number of collected grains is likely to be as low as 10 per day on the exposed target. The effective area over which the beam can be deflected while retaining adequate secondary ion collecting efficiencies is  $200 \times 200 \mu\text{m}^2$ , so that the complete exploration of the  $10 \times 10 \text{ mm}^2$  target by the primary ion beam would require 2500 displacements of the target and would consume a large percentage of the beam time. The target imaging device, COSISCOPE, will image an entire  $14 \times 14 \text{ mm}^2$  area holding one  $10 \times 10 \text{ mm}^2$  target with a magnifying power of 1 on its  $1024 \times 1024$  pixels, which gives a pixel resolution of  $13.7 \mu\text{m}$ . Each target will be imaged before and after exposure and will provide a list of coordinate positions where collected grains are most likely to be found. In addition, COSISCOPE is useful to monitor the evolution in time of targets coated with very fluffy material and to verify the accuracy and reproducibility of the target positioning by the Target Manipulator Unit.

COSISCOPE is contributed by the group at IAS, Orsay, France, and uses copies of the units developed for the ÇIVA camera system onboard the ROSETTA lander to save both, mass and volume. The CCD is part of a three-dimensionally integrated 'camera-head'. The processor unit is built around a DSP-21020 operating at 20 MHz with 6 Mbytes of RAM and two FPGAs for the interfaces. The command and data interface with the COSIMA CDPUs is a pair of RS-422 serial lines, which can operate at up to 10 MHz. The total mass is 460 g including the mechanical structure and the optical elements.

Particle detection on metal black is difficult for two reasons: First, the albedo of the target surface is low, as is the expected albedo of a major fraction of cometary grains. Second, the targets have a surface roughness at scales comparable to the COSISCOPE resolution. Illumination by a red LED (650 nm) at a low incidence ( $5^\circ$  to  $10^\circ$  above the surface) has proven to be effective to detect surface inhomogeneities. A second image, obtained by a LED from the opposite direction, improves the

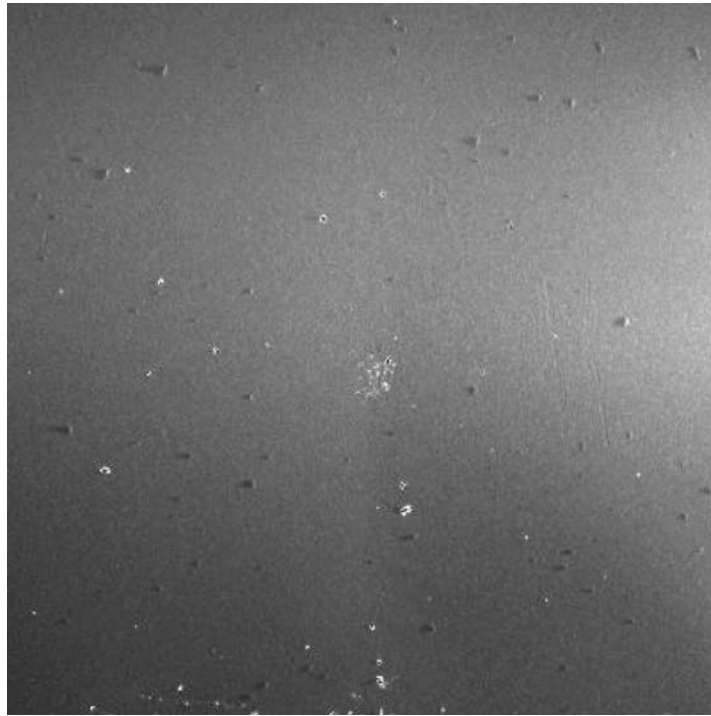


*Figure 8.* COSISCOPE image of a  $2 \times 2$  mm<sup>2</sup> region on a collector substrate exposed to silicate dust. The low incidence light comes from the right. A cluster of silicate particles is visible in the center. Other dark ‘low velocity’ grains stick on the surface with long shadows extending to the left. The bright spots are scratches or blank metal particles from the (early) production process. The noise level from the substrate is acceptable even under shallow illumination.

detection quality. The grain detection algorithm takes advantage of the higher bidirectional reflection coefficient of the grain’s side facing the LED when compared to the surface (even with the same low albedo), which provides a contrast with the shadow of the grain if it sticks out of the surface (see Figure 8 for an example). This approach is not so efficient for very fluffy aggregates, which are spread out over several pixels, but such features are still expected to provide a signature by increasing the local roughness. The output of the process is a series of messages to the COSIMA main processor with a list of features, each with its coordinates, size, and a quality index (based on a combination of criteria such as the observed contrast and the correlated detection with both LEDs). This list of features can be used on board and on the ground to define regions of interest to be analyzed.

The coordinates are calculated with reference to two pairs of  $50\mu\text{m}$  sized reference dots at a distance of 5 mm on the calibration strip of the target holding assembly where the metal underneath the black has been exposed using laser blow-off (Figure 9). This allows COSISCOPE to monitor target positioning by the TMU

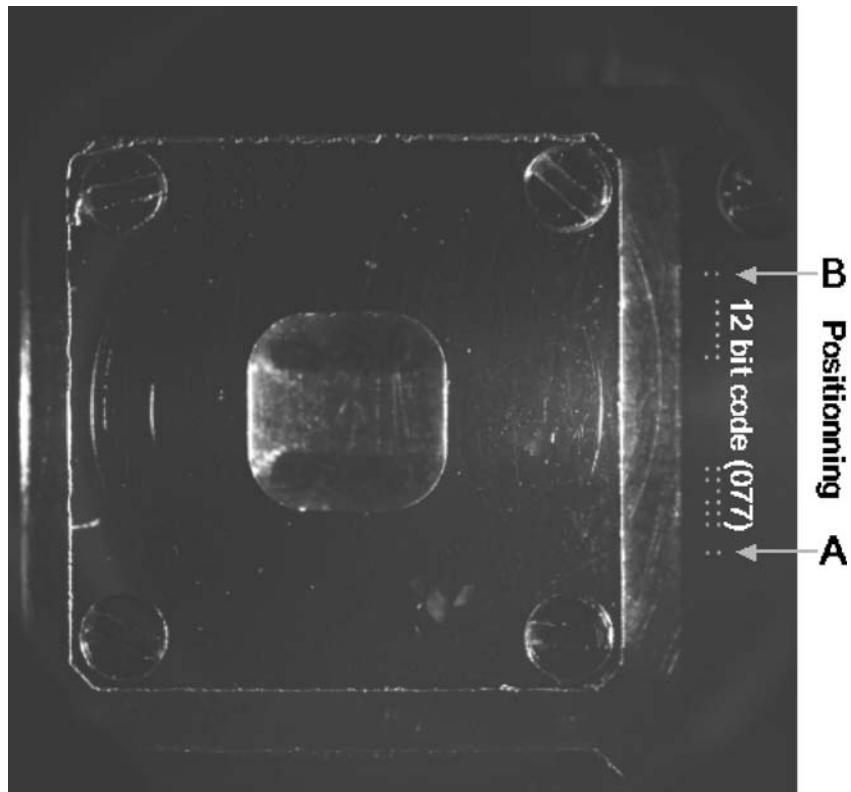


*Figure 9.* COSISCOPE image of a collector substrate obtained during the in-flight commissioning phase in September 2004. Two pairs of  $50\ \mu\text{m}$  dots with a  $200\ \mu\text{m}$  interval (A and B) on the calibration strip of the target assembly are separated by 5 mm. They are used by COSISCOPE to monitor the position of the target assembly in its field-of-view. After defining the target reference frame from the positioning pairs of dots, COSISCOPE checks the two groups of dots, which defines a 12 bits code (2 dots: 1; 1 dot: 0), here '00001110111' from top to bottom, or '077' in hexadecimal format.

with an accuracy of less than  $10\ \mu\text{m}$  by comparing the nominal and observed position and angular orientation of the target in the COSISCOPE field of view. A 12 bit code constituted of two sets of six bits makes it possible for COSISCOPE to identify the target. The positioning and labeling information is sent to the ground together with the feature list, whether or not an image is transmitted, to monitor TMU operations.

The full COSISCOPE power cycle for one operation takes less than 20 s with a mean power of 4 W. A specific COSISCOPE calibration mode allows transmission of the actual image, compressed by a factor of 10, using a wavelet transform with tree-coding algorithm, as well as the associated list of features. COSISCOPE calibration sequences will be performed during in-flight instrument checkouts, at the beginning of the main encounter phase, and then upon request, e.g., every few

weeks to select the COSISCOPE operating parameters for the following measurement slot.

### 3.4. THE PRIMARY ION BEAM SUBSYSTEM (PIBS)

#### 3.4.1. *Functional and Performance Requirements*

The PIBS, contributed by the group at the LPCE, Orléans, France, needs to perform to the following specifications to enable COSIMA to achieve its scientific objectives:

It has to provide a pulsed and focused beam of ions with the following properties:

- $^{115}\text{In}^+$  ions,
- at 8 keV,
- about 1000 ions per pulse,
- within an elliptical focal spot of less than 20  $\mu\text{m}$  major axis,
- within 3 ns,
- to a location within 100  $\mu\text{m}$  of the optical axis of the COSIMA extraction lens,
- at a repetition rate of up to 2000 ion pulses per second.

The ion emitters are provided by the Austrian Research Center in Seibersdorf, Austria, while the IWF in Graz, Austria, provides the emitter power supplies and control electronics.

#### 3.4.2. *General Concept*

To achieve the above specifications, PIBS has a sophisticated ion optical concept, using fairly simple elements to keep the mechanics simple. It is shown in Figure 10 as schematic and in Figure 11 as picture. The ions are generated in one of two liquid metal ion sources, filled with isotopically clean  $^{115}\text{In}$  (>99.9%) and accelerated into the ion optics by the same electrical field. Two separate emitters are implemented for a limited redundancy. During normal operation, one emitter is used for sample analysis, the other for target cleaning (by ion sputtering). Only one emitter can be operated at a time. Should one of the emitters fail or exhaust its indium reservoir, the backup mode can be chosen, in which the electrostatic switch allows transfer of the beam of either emitter to the respective other side.

On the analyze channel, a first lens LA1 (or LC1 in the backup configuration) gives an image of the emitter in the inlet plane of the chopper, then a second lens LA2 builds the final image on the target. The chopper consists of two pairs of short blades generating a transverse electrostatic field on the beam path between them in order to divert the beam to a screen. For analysis, the field is cut for 50 ns, and a beam packet is generated on the normal beam path. This packet is then compressed by a buncher into the short pulses required on the target. The actual buncher requires three stages due to the voltage limits imposed by the available electronic flight parts. In each buncher stage, a pulsed longitudinal electrostatic field is applied between

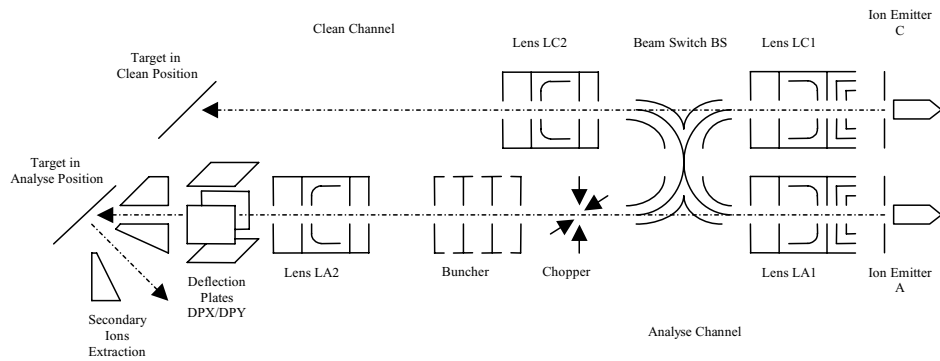


*Figure 10.* Schematic sketch of the Primary Ion Beam Subsystem design: Ions from two emitters at the right side can reach either of two positions: ‘Analyze’ or ‘Clean’, depending of the ‘Beam Switch’ in the center. The focusing elements are electrically shared, as only one beam can be active at any time. ‘Chopper’ and ‘Bunchers’ provide the pulsed beam for analysis, the deflection plates are used for steering the beam spot on the target.

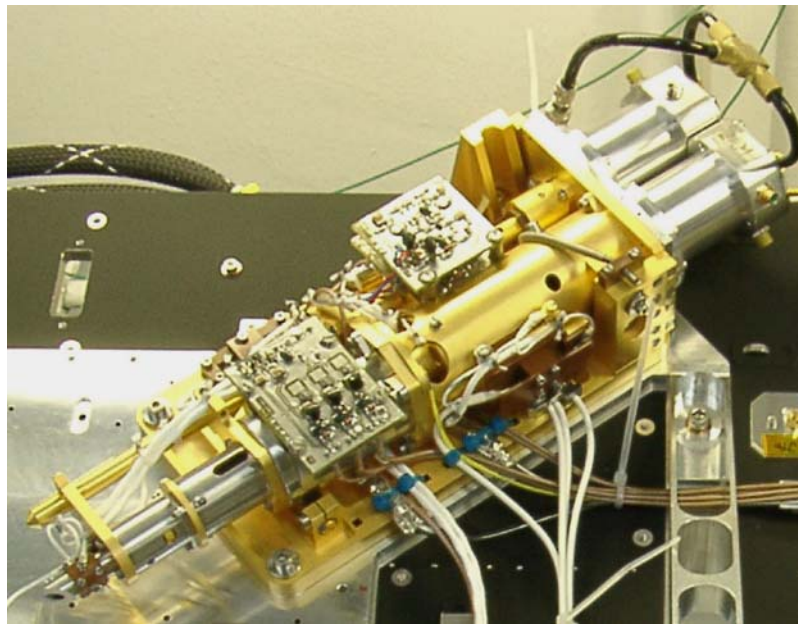


*Figure 11.* The COSIMA Primary Ion Beam Subsystem during integration at vH&S Schwetzingen, Germany (Photo vH&S): Note the amount of wiring to make the unit operational and yet keep it free from contamination.

two parallel electrodes at the time when the ion packet is completely between them. Typically, a potential of +250 V is applied to the upstream plate, once the ion packet has passed it. As a result, ions at the trailing end of the packet gain additional energy and ideally meet ions of the leading edge exactly at the target. Two orthogonal sets

of two parallel deflection plates are used to control the position of the beam on the target in both, horizontal and vertical directions. The horizontal deflection plane has been chosen to coincide with the deflection plane for the corresponding system for the secondary ions.

The other ion beam used for cleaning has a first lens LC1 (or LA1 in the backup configuration), which gives an image used by LC2 to build the final image on the target in the clean position. The ion beam for cleaning is not pulsed. This fact allows also a rapid sputtering of the sample (at about 1 monolayer/s) in order to make a measurement at a different depth (accepting the degree to which the sputtering does modify the sample).

The lenses LA1, LC1, LA2, and LC2 are three-electrode electrostatic lenses in the Einzel configuration. Their structure is chosen to minimize the spherical and chromatic aberrations. This is especially important for lenses LA1, LC1, and LA2, which are used in the analysis process. Since only one beam is active at any time, the lenses of groups '1' and '2' are connected in parallel.

### 3.5. THE SPECTROMETER ION OPTICS

The combination of SIMS and TOF methods places particular constraints and requirements on the ion optical system:

1. It is important to collect for analysis the maximum fraction of secondary sample ions produced by the primary ion impacts, which is normally achieved by using an electrostatic lens.
2. It is necessary to have low geometrical aberrations in the focusing lens so that the accelerated ions all hit the detector after passing through the drift region (small geometric aberration).
3. It is necessary that the ion optics does not add time dispersion to the ions' flight time due to the different electrical fields along the differing paths of the secondary ions during acceleration and focusing (small time dispersion).
4. The ion optical system must neutralize the effects of the initial energy distribution of the secondary ions, which adds time dispersion to the flight time and thereby limits the mass resolution (time compensation for initial energy).
5. As many of the ions as possible that enter the system should arrive at the detector (high transmission).

Design and optimization has been done by the CoI, N.G. Utterback, Santa Barbara, USA, using the SIMION software package (Dahl, 1997). The design was driven by the rule that as few elements as possible would be required. The extraction lens has an internal field stop and images the 100  $\mu\text{m}$  source area onto the 30mm detector. No further lenses are implemented. The following sections will describe the COSIMA ion optical system as to how and how well these requirements have been met.

### 3.5.1. *Secondary Ion Extraction and Focusing Lens Elements*

The dust samples (cometary dust particles) are collected on electrically conducting surfaces. During analysis, as shown schematically in Figure 1, one of these targets with the dust sample on its surface is placed 3 mm from the extractor electrode entrance with an aperture of 2 mm in diameter. The target is maintained at ground (0 V) potential. The extractor electrode is maintained at  $-3000$  or  $+3000$  V (for positive or negative ions, respectively). The remainder of the ion optical system is biased to  $-1000$  V or  $+1000$  V to maintain an ion kinetic energy of 1000 eV in the drift region. The focusing lens elements follow the extraction aperture and consist of apertures producing two highly non-uniform, but radially-symmetric electric field regions. Between these regions is an aperture that limits the diameter of the beam at that point and has the effect of eliminating ions that have too high initial energies and angles. If not eliminated, these ions would follow large off-axis trajectories that would cause unacceptable geometric aberrations and time dispersion. The length of the lens elements from extractor surface to lens exit aperture is 15 mm. Immediately following the lens components is a deflection region with 2 sets of parallel plates, 25 mm long and set perpendicular, that are used to deflect the beam to compensate when the primary ion beam is scanning at an off-axis position. Without this compensating deflection, the lens magnification of the target region (lens object) would cause the secondary ion beam to miss the detector. The first drift region measures 540 mm from the lens exit aperture to the entrance grid of the ion reflector.

### 3.5.2. *Ion Reflector for the Compensation of Initial Ion Energies*

The distribution of the initial energy of the sample ions, resulting from the formation mechanism, causes ions of the same mass to arrive at a given distance at different times. This puts a limit on the mass resolution of TOF instruments. Without initial ion energy compensation, COSIMA would be limited to a mass resolution  $m/\Delta m$  well below 100. Since the investigation needs a resolution  $m/\Delta m$  of several thousands, initial ion energy compensation must be provided. Mamyrin *et al.*, (1973) have shown that a two stage reflectron has the capacity to achieve this. From their analysis it follows that the ion reflector must have two sections with different electric fields, one to retard the ions and a second one for the actual reflection. This allows compensation of the effects of the initial energy up to the second order in  $dE/E$  (initial energy/given energy). However, the appropriate drift path length, the retarding region path length, and electric field strengths depend on the magnitude of  $dE$ . Hence, the effectiveness of the initial ion energy compensation will depend on the initial ion energy distribution, and the parameters must be set for the best compromise for a given initial ion energy distribution. The COSIMA 2-stage reflector consists of the interior of a cylindrical region, 50 mm in diameter and 70 mm long. Three planar grids with 91% transmission and the solid end cap define the two electric field regions. The entrance grid defines the end of the first drift region. 20 mm beyond the entrance grid, the second 'retarding' grid defines the end of the

retarding region and the beginning of the reflection region. The third ‘reflecting’ grid another 40 mm beyond defines the end of the reflection region. The end cap 10 mm beyond is biased with respect to the third grid in order to trap any ions and electrons produced by impact of neutrals on the end cap. The uniform electric fields are produced by 14 cylindrical conducting rings, which are plated onto the inner surface of the cylindrical region. In the first deceleration region, the ions are slowed down from a kinetic energy of 1000 eV to 200 eV. A potential difference of about 290 V is placed between the grids defining the reflection region. This potential difference is varied to ‘tune’ the initial ion energy compensation so that ions of a given mass arrive at the detector with the minimum time dispersion possible. All these voltages can be modified by telecommand and an internal optimization routine, just to accommodate unexpected effects during flight.

After the reflected secondary ions exit the reflector, they travel in a field-free region for 510 mm before passing through the entrance grid of the ion detector. Discussions of the ion detector and electronic amplifiers and counters are covered elsewhere (see 3.6).

### 3.5.3. *Secondary Ion Optical System Design Properties and Results*

The design properties and results presented here are based on computer simulations, which are in turn based as closely as possible on the flight mechanical and electrical configurations, and the expected parameters for the physical processes involved. The computer simulation program was SIMION by Dahl (1997). The largest unknown in the simulations is the initial energy distribution of the secondary ions and their initial emission angular distributions. A further parameter, which is likely to be important, but is very hard to simulate accurately, is the effect of sample (collected dust particle) size and shape as it resides on the target surface. The simulation assumes that target and sample are co-planar and, hence, yields the best case in terms of time resolution. The actual finite sample size may degrade the time resolution, but only laboratory investigations can then show how and by how much. For the results presented here, a Maxwell-Boltzmann energy distribution with  $kT$  of 10 eV was assumed for the secondary ion initial energy distribution. A  $\cos \vartheta$  angular distribution was assumed for the secondary ion emission angles. Other values for  $kT$  were also tried, as well as comparing a  $v^4$ -angular distribution, with results not markedly different in terms of COSIMA requirements. The primary beam is taken to have a Gaussian radial distribution with  $\sigma = 10 \mu\text{m}$  and strikes the target at  $40^\circ$ . Here the actual laboratory measurements and the SIMION results compare very well. The transmission of the secondary ion optical system for the flight configuration (limiting aperture in focus lens of 1.2 mm diameter) is found to be 21%. Transmission is defined as the number of secondary ions that reach the detector divided by the number of secondary ions produced at the target. It may be noted that 4 passages through 91% transmission grids already limits the transmission to 68%. The remainder of the ions lost strike the lens electrode outside the limiting aperture. The lens focusing quality is such that all ions strike the detector

within a circle with a diameter of 15 mm, which is well within the effective area of the detector. This includes the slight scattering due to the high field strengths near the grid wires, which is accurately simulated. The distribution of flight times for 25000 ions of mass 100 is approximately a Gaussian with  $\sigma$  of 1 ns, equivalent to 2.2 ns FWHM (full width at half maximum). There were no flight times outside a window of 5.5 ns. The distribution was centered at 31.037 microseconds. This corresponds to a value for  $t/\Delta t$  of 14000, which yields a mass resolution  $m/\Delta m$  of 7000 based on the FWHM criterion (it should be noted that  $m/\Delta m$  is one half of the  $t/\Delta t$  value). This flight time dispersion is due to the remaining uncompensated effects of the initial secondary ion energy as well as the different paths traversed through the high electric fields in the focusing lens. The latter effect is controlled by the limiting aperture within the focusing lens. In order to gain maximum transmission, the limiting aperture is chosen as large as possible without introducing unacceptable time dispersion. The flight time and spatial distributions widen slightly and the transmission decreases slightly when the primary ion beam is scanned off the lens axis at the target, but the effects are within about 15% for primary beam scanning up to 100 microns off the lens axis. It needs to be noted, that the mass resolution  $m/\Delta m$  of 7000 is for the ion optical system only, and assumes that all secondary ions start at the same time (effectively achieved for high masses  $>3000$ ). In reality, the primary ion pulses will have a time dependence which is roughly Gaussian with FWHM of order 3 ns. At mass 100 the actual  $m/\Delta m$  is about 2000.

### 3.6. ION DETECTION

Once the ions reach the end of the outgoing drift tube, they need to be detected with high time resolution. For this purpose a detection unit with high gain for single ion detection, a time resolution of about 1 ns, and an active area of about  $5 \text{ cm}^2$  is required. Proven solutions are built on microchannel plates (MCP) or more recently on microsphere plates (MSP). We decided to use a MSP from EMUL because of its greater mechanical robustness and its higher gain, which leads to a single element solution with a 1.4 mm plate. The detector design is shown in Figure 12. Its elements are from top to bottom: the entrance grid at drift-tube potential, the intermediate grid to apply the post acceleration potential, the microsphere plate, the anode plate with capacitive coupling to the board with the trigger electronics. As the COSIMA target is always at ground potential, the potentials within the ion detector also refer to ground. Their values differ for positive or negative ions, they are not symmetrical to ground, and range up to more than 12 kV (see Figure 12 for details). This demonstrates the insulation needs associated especially with the negative ion case, which had to be solved within the very small volume available. The capacitive coupling of the detector output signal is an elegant and effective way to keep the associated detector electronics at ground potential. It actually represents two high quality coupling capacitors: C1 for the coupling to the trigger circuit and C2 for

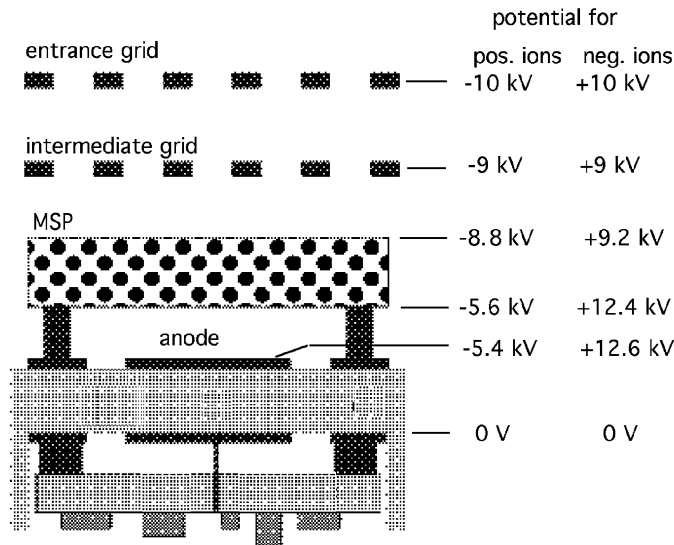


Figure 12. The COSIMA ion detector unit. The COSIMA ion detector is a complex arrangement with many grids and different high voltage values within a small space. An amplifier is integrated for low noise and high signal.

the signal return path. Due to the low parasitic inductance of the design, the fast output pulses are without significant ringing. The typical pulse height distribution of this detector is well determined and shows a typical gain of  $10^7$  for a MSP supply voltage of 3200 V. The shape of a typical MSP output pulse is shown in Figure 13. It was measured with an oscilloscope of 1 GHz bandwidth. The FWHM of about 1 ns and the signal rise time of less than 0.8 ns are quite adequate for COSIMA. The MSP output is coupled directly into the detector electronics through the capacitor, which also provides high voltage insulation. The electronics has to discriminate the output signals above a given threshold against noise background below this threshold. The pulse height distribution shows a distinct level for this threshold. Any change due to, e.g., aging of the MSP can be adjusted by changing the operational voltage applied to the MSP. The electronic pulses need to be standardized in both, amplitude and pulse width. As the rise time of the MSP pulse is less than 1 ns, a leading edge threshold trigger with a fixed threshold is sufficient to process the signal. The maximum principal time error caused by different pulse amplitudes is then also less than 1 ns. For a supply voltage of 3.2 kV a threshold charge of 2 to 5 pC is appropriate to separate ion signals from noise. For pulses with a width of about 1 ns, this results in peak currents in the range 2 to 5 mA. The direct coupling of the electronics avoids signal ringing due to, e.g., unmatched lines. The output feeds a 50  $\Omega$  terminated coaxial line with 200 mV amplitude and 5 ns pulse width. The length can be chosen within reasonable limits. The circuit is supplied with a single supply voltage of nominally  $-5$  V and a worst-case power consumption of  $P_{\max} = 75$  mW. Laboratory tests suggest that changes of the supply voltages

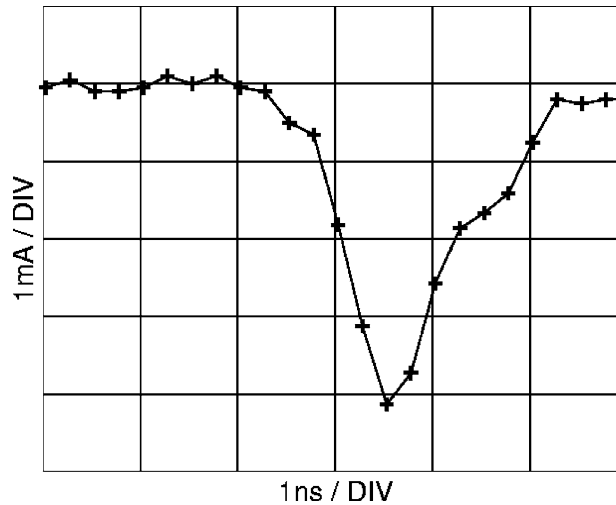


Figure 13. MSP output pulse. A typical output pulse from the microsphere plate shows the good signal quality and trigger properties achieved. The pulses are fast enough for the COSIMA timing requirements.

could be compensated with an adjustment of the MSP gain through its operational voltage, while temperature changes of several 10 K do not matter.

### 3.7. ELECTRONICS

The COSIMA electronics contains all necessary elements to control and operate COSIMA. It is also home to those components contributed by other groups. All electronics are housed in the electronics box with the exception of a few fast switching circuits of PIBS. This is done to prevent any outgassing products to directly interfere with the high sensitivity TOF-SIMS instrument. An overall block diagram of the COSIMA experiment is shown in Figure 14.

#### 3.7.1. Power Supply Electronics

The COSIMA experiment operates from a single power line of nominally +28 V from the ROSETTA S/C power subsystem. A low-voltage supply unit within COSIMA, built from a set of switching DC/DC converters and a linear regulator, provides the main low voltages +15 V, +5 V, -5 V, and -15 V for supply of the experiment subsystems. The output power lines for the TMU, the COSISCOPE, and all HVCs are routed through a low-voltage switching unit. This unit allows some power management as the power budget of COSIMA does not allow simultaneous operation or even idling of all of its components. Switching is executed under software control through the experiment processor system. An optoelectronic device senses the power line from the spacecraft. Once it drops below a certain value, an interrupt is generated and the processor system will save the current settings of the

COSIMA – HIGH RESOLUTION TIME-OF-FLIGHT SECONDARY ION MASS SPECTROMETER

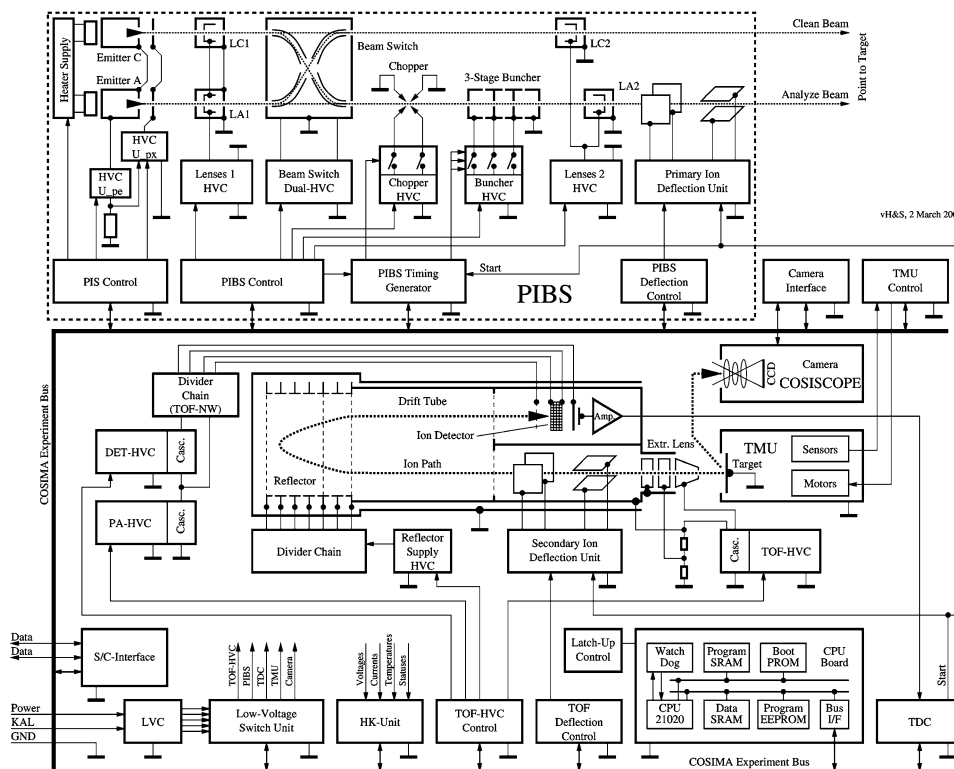


Figure 14. COSIMA block diagram. This full block diagram of COSIMA demonstrates the complexity and the predominance of the high voltage power supplies, which ultimately make COSIMA a very versatile instrument.

COSIMA operational parameters and try to shut down the instrument orderly, as long as secondary power lasts.

The multitude of ion optical elements of COSIMA requires a large number of high voltages, five for PIBS, two for the indium emitter, and five for the spectrometer, with their voltages being individually controlled through the instrument processor. Most of these voltages must be stable to  $10^{-4}$  with respect to temperature and time, and must have a similarly low ripple. Otherwise the spectra would be badly affected and the mass resolution and mass identification would be lost. Therefore, a set of high voltage converters were designed based on a concept used for the CoMA/CRAF and the CIDA/STARDUST instruments. The converters are of ‘Royer’ type, optimized for precision and low power consumption. They are synchronized to subharmonics of a quartz oscillator frequency, so that their low EMC radiation is within fixed frequency bands specified by the project. Their feedback is achieved by pulse width modulation. The first high voltage stage is built from a step-up transformer, whereas the full voltage is generated through high voltage cascades.

### 3.7.2. Time-of-Flight Measurement

The total flight time, which is the time from the formation to the detection of an individual secondary ion, is the basis for the TOF spectrum, and, hence, the mass spectrum. For COSIMA, the start time for all time measurements is the chopper pulse for the primary ion beam. The time interval due to the flight time of the primary ions from the chopper to the target is an unavoidable offset to the flight time of the secondary ions. Each detector pulse is the ‘STOP’ signal for the flight time interval of an individual ion. The required mass resolution and total mass range necessitate a time resolution of about 2 ns and a measurement range of 250  $\mu$ s. An additional requirement is a short dead time, i.e. the time interval during which two ‘STOP’ signals cannot be processed. The number of secondary ions per primary ion pulse can vary over a wide range, but 1000 has been accepted as a reasonable upper limit. Each of these time intervals has to be converted to a digital number. The time-to-digital converter (TDC) satisfying these requirements is designed in a completely digital form, for which most of the parts are included in a high reliability Field Programmable Gate Array (FPGA) from ACTEL.

The TDC has a 13 bit clock counter fed by the master clock with a period of  $T_{\text{clock}} = 31.25$  ns, which gives a total measurement range of 256  $\mu$ s. Within each clock period, a 16 stage interpolation leads to an overall resolution of about 1.95 ns. This interpolation is done by a time-to-position transformation using a ‘tapped delay line’, which is actually set up by 16 non-inverting CMOS buffers. Of course, the total propagation delay of the delay line has to be equal to one clock period. As the master oscillator is used for the PIBS timing too, the start signal is synchronous avoiding additional errors in the time measurement. The propagation delay is then the only critical parameter. It has to be adjusted to match exactly the length of one clock period. This is effected through the supply voltage. To do this, a simple calibration routine is run under processor control. The result is subjected to a statistical analysis of the times of randomly generated pulses. This way no precision calibration pulses need to be generated. Once all time bins are filled equally the adjustment is correct. In flight the calibration routine is selfcalibrating to compensate temperature induced drifts of the electronics.

Figure 15 shows a simplified block diagram of the TDC. The input signals from the detector unit are fed into the delay line. The taps are sampled with the rising edge of the master clock. If a ‘STOP’ pulse is detected within the sampled bit pattern the 16 tap signals and the value of the clock counter  $C_{\text{clock}}$  are stored into a fast first-in-first-out memory (FIFO), which can hold about 3000 ‘STOP’ entries. The experiment processor reads the data from the FIFO memory asynchronous at a lower speed.

The principle of the time-to-position transformation is shown in the Figure 16. An incoming ‘STOP’ pulse propagates through the delay line with a speed of one tap per 1.95 ns. All taps are sampled simultaneously at the edge of the master clock, i.e., at the time  $C_{\text{clock}} * T_{\text{clock}}$ . For a leading edge of a ‘STOP’ pulse at position P within the sampled bit pattern the time of arrival can be calculated to be

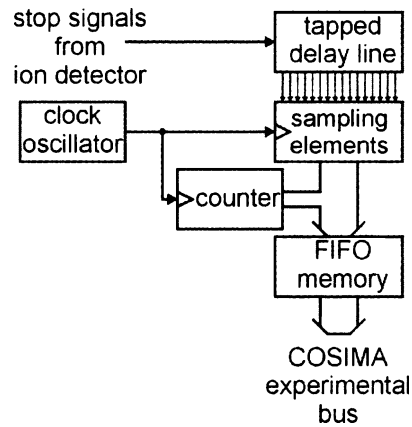


Figure 15. TDC Block diagram of the COSIMA time-to-digital Converter: The data from the tapped delay line and the master clock counter are added and stored in a hardware device until the instrument's processor can pick up the data.

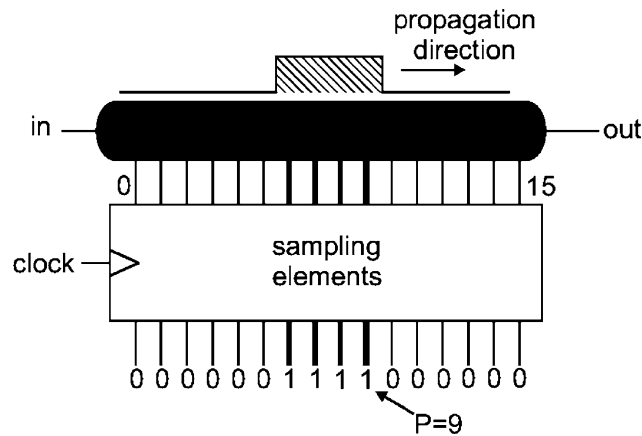


Figure 16. Time-to-position principle. The pulse from the detector amplifier moves from left to right through the delay line and, at a given time, is detected by several elements. The '1's are later interpreted by the software to derive the exact time of the event.

$t_{\text{arrival}} = C_{\text{clock}} * T_{\text{clock}} - P * 1.95 \text{ ns}$ . Once the position of the leading edge has been determined by the software, it can be decoded to a 4 bit number. Together with the 13 bit counter value, there are 17 bits corresponding to  $2^{17} = 131072$  time bins. More than one 'STOP' pulse may occur within 32 ns and be inside the delay line at the same clock cycle. Such a case defines the dead time as the minimal distance between the two leading edges. It turned out, that for the proper function of the delay line the pulse width had to be increased to 5 ns, which results in a dead time of about 10 ns.

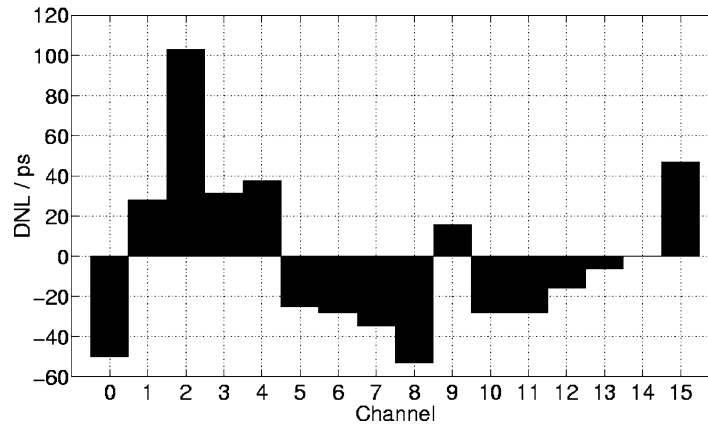


Figure 17. Differential linearity of TDC. The measured differential non-linearity of the system is an order of magnitude smaller than the COSIMA time-of-flight resolution.

The accuracy of the 2 ns delay steps is well defined and can be measured onboard using the calibration. Figure 17 shows the differential non linearity (DNA), which was measured for the 16 interpolation channels. The DNA is the deviation of the step width of one channel and is better than 120 ps for any channel which is much better than the nominal 0.5 LSB (Least Significant Bit) DNA. Thus all 17 bits are valid for the analysis of flight times.

### 3.7.3. Instrument Control

As is state-of-the-art, instrument control for COSIMA is provided by a microprocessor-based system (see below). Two categories of control are implemented, a digital subsystem transferring information on the system bus and an analog subsystem serving individual control lines. The dedicated, more complex units like COSISCOPE, and, to a lesser degree, the Target Manipulator Unit, and the Primary Ion Beam System are globally controlled, as they have some of the control functions residing within them. A general overview of the state of the instrument is maintained by continuous monitoring of the standard housekeeping values. The functions of PIBS and TOF are controlled by 20 adjustable high voltages. Apart from a collective ‘disable’ of all high voltage generators, these can be controlled by variable analog voltages in the range 0...10 V. (For all high voltages the voltage is controlled, except for one case: the extraction electrode of the primary ion source, where the emission current is monitored.) The high voltage settings need a resolution of 12 bits and very good stability over temperature and time. Generating these by 20 individual digital-to-analog converter ICs would have required a large amount of hardware. Instead, a simpler solution was found: A single PGA generates twenty pulse-width modulated square wave signals with a fixed frequency of 9 kHz. The duty cycles of the square waves are set under processor control between

0% and 100% with 12 bit resolution, where the LSB is generated by noise-shaping. The constant amplitude of the square waves is precisely given by a stable reference voltage source. The DC levels, which are proportional to the respective duty-cycle, are built by lowpass filtering of the individual square waves. Besides the values of the high voltages, their polarity in the TOF section and actual values in the PIBS need individual adjustment for either positive or negative secondary ions. Special precautions are needed when altering the polarity. This is done through the use of bistable relays. The control of the high voltage polarity lines has to be consistent with the control of the bistable relays, which switch between HV cascades for the positive and the negative case. Further more, these switching operations are only safe while there is no high voltage present, otherwise high voltage discharges could result in contact damage. Therefore, the control was set up in a hardware state machine, which also forces the relay coil drives to be consistent with the high voltage polarity control line setting before the high voltage generators can be enabled. It further sequentializes driving of the bistable relay coils to reduce the total coil current.

#### 3.7.4. *Data Collection*

Two types of data are collected within COSIMA and both are needed to properly interpret the measured time-of-flight data: slow, housekeeping-like data such as settings of the actual voltages for the PIBS and the TOF section, positions of the targets and features thereon, and the fast arriving time-of-flight data for the secondary ions after a primary ion pulse. As discussed above, the fast data are accumulated at instrument speed in a FIFO, from where they are read at processor speed. The detailed timing is executed from hardware registers. Conflict may arise, when after 1000 (tbd) primary ion pulses the arrival data are assigned to their respective time bins. During this process the timing performance is verified by checking the position and width of the hydrogen ion peak (for both positive or negative ions), as well as for another (yet to be determined) mass line. Deviations above a certain limit will lead to the readjustment of operational voltages to keep the mass lines in the same bins throughout an entire analysis, which may last for several hours (rather than to use extensive recalculation of mass values to the time bins). During such phases of intense calculations, the instrument may continue to measure for the next 1000 primary shots, or its operation is halted and the primary ion emission is reduced until the end of the calculations. This task can be scheduled in flight taking into account actual performance and temperature change rates.

Once there are enough data of non-hydrogen secondary ions accumulated (typically a few thousands), the quality of the respective site is analyzed using code derived from chemometric methods (see 3.8 below). The data and the results of the analyses are then packed into an experiment data frame and sent to telemetry for transmission to ground.

### 3.7.5. *The Instrument Processor System and Latch-up Control*

The COSIMA instrument is entirely under the control of its processing unit. The CPU board is built to accommodate the instrument's computational and memory requirements. The board is built around a floating-point digital signal processor (DSP), type ADSP 21020 from Analog Devices, in a radiation-hard version built by Lockheed Martin Federal Systems running at 16 MHz. This signal processor has a Harvard architecture, with a 48 bit program-data bus and a 32 bit data-data bus.

The experiment software is stored in two EEPROMs of 128 kByte each. During the power-up procedure the program code is copied by the boot-loader, residing in three radhard 8 kByte PROMs from Harris, into the program RAM of six radiation tolerant 512 kByte CMOS SRAMs, from where it is later executed. The data memory is built from another four 512 kByte SRAMs, which allow processor operation with 32 bit IEEE floating-point numbers.

For permanent storage of the experiment setup and status information during times, when COSIMA is not powered, a 128 kByte SRAM is constantly supplied by a separate DC line from the S/C. This 'keep alive' memory allows quick reconfiguration of COSIMA after, e.g., a power drop or software stall.

The CPU board controls the COSIMA electronic boards through a synchronous 16 bit wide I/O bus with 256 possible addresses. The bus control by the CPU board is achieved through a combination of 'valid-memory-address', 'read', and 'write' signals. High bus reliability is obtained by synchronous timing circuits on the CPU board, which insert wait-states on the I/O bus to give long data hold times during write.

Since the memories on the CPU board are rad-tolerant but not single-event latch-up proof, a latch-up protection circuit is on the CPU board. The board is subdivided into areas, for which the individual supply currents are monitored. If a latch-up condition occurs, the supply current increase in one board area is immediately limited by an on-board current limiter, which protects the memory ICs from destruction. At the same time the power supply of the CPU board is completely switched off, so that the latch-up condition dies out. After a delay of a second, the CPU board is powered up again, and the boot-up procedure starts. The occurrence of a latch-up condition can then be deduced from the last experiment status stored within the keep alive memory.

### 3.7.6. *On-Board Data Handling and Telemetry*

The COSIMA software consists of two distinct parts: the boot-ROM code and operational code. The boot-ROM resident code provides for the following tasks:

- appropriate instrument setup at power up
- handling of all the ROSETTA S/C telecommand and telemetry services
- loading the operational code from the EEPROM or from the S/C.
- safe mode operation and recovery, if the operational code fails
- basic instrument housekeeping

The operational code provides all the functionality of the instrument. Individual operations are handled through interpreted code (like in the FORTH-language), which in turn calls compiled and optimized lower level subroutines.

The use of an interpreter gives more flexibility to both, updates of the software during the long mission, and it also provides a simple multitasking environment.

All of the operational code is written in relocatable modules. Should one part of the memory fail, the code can be transferred into another section. In addition, the modules can be updated individually. The interpreter calls the subroutines through jump tables so that individual tasks can be arranged by simply composing the proper jump addresses.

### 3.8. ON-BOARD PRE-EVALUATION

Basically COSIMA produces time-of-flight spectra. The data for each primary ion pulse are added into time bins. After about 1000 shots the data should be significant for a first evaluation to characterize the site under analysis. For this purpose the time bins are scanned for peaks at the known locations of mass lines of interest. With the expected mass resolution of  $m/\Delta m > 2000$  (FWHM), several peaks may appear for each integer mass number, representing atomic and molecular ions (e.g.,  $K^+$  and  $C_3H_3^+$  for mass number 39). Since cometary grains are a complex mixture of inorganic and organic compounds, this high-resolution data treatment is essential. Two peak lists are generated containing the absolute peak intensities (number of ions) per integer mass for both, inorganic and organic ions. These lists are used for further data evaluation. Although the mass resolution is not sufficient to determine the sum formula of an ion by discriminating isobars (e.g., triazine  $C_3N_3H_4^+$  at 82.03997 amu from pentdienimine  $C_5NH_8^+$  at 82.06513 amu), the dominating ion type can be determined by line position analysis (i.e., at which exact mass value most of the ions are found). An automatic comparison of peak list tables is necessary for the detection of cometary grains (target vs. grain signals) or to decide whether a newly measured site differs from those already analyzed. The strategy for comparison of organic spectra is as follows: Several similarity criteria will be used, and transformation of data (prior to comparison) will be applied. The aim of transforming the original data into a set of features is to achieve a better representation of the chemical structure in the mass data. A spectral feature is a numerical variable that characterizes a spectrum; it is a linear or nonlinear function of all or selected peak intensities. Varmuza *et al.* (1999, 2001) and Werther *et al.* (2002) have tested different types of spectral features using data that are similar to TOF-SIMS data. They found that promising concepts for feature generation for organic compounds are (1) intensities at selected masses, (2) intensities averaged in selected mass intervals, (3) logarithmic ratios of selected intensities, (4) summation of intensities at fixed mass differences (e.g., 14: modulo-14), and (5) autocorrelation.

Let  $x(i, A)$  and  $x(i, B)$  be spectral feature  $i$  for mass spectrum A and B, respectively, scaled to the range 0 to 100. Similarity criteria can be defined for instance

as following (summation over all  $n$  selected features):

$$S_1 = \sum [x(i, A) * x(i, B)] / \left\{ \sum [x(i, A)^2 * \sum [x(i, B)^2] \right\}^{0.5}$$

correlation coefficient [0 . . . 1] (2)

$$S_2 = [1/n] \sum [x(i, A) - x(i, B)]^2 \quad \text{mean squared error [0 . . . 100]} \quad (3)$$

$$S_3 = \left\{ \sum [x(i, A) - x(i, B)]^2 \right\}^{0.5} \quad \text{Euclidean distance [0 . . .]} \quad (4)$$

Promising concepts for feature generation with mineral spectra are: (1) intensities of the major isotopes of atomic ions (which may turn out to be not so simple as they can be masked by molecular ions as, e.g.,  $m = 24$  amu can be superimposed by Mg and C<sub>2</sub>), (2) intensities averaged over all isotopic contributions of atomic and molecular ions (again with the ambiguity that several isobars may additionally contribute in these mass intervals), (3) linear and logarithmic ratios of intensities (mainly for isotopic and for some crystal order analysis), (4a) modulo-4-summation (total contribution of the main isotope ions from minerals), (4b) modulo-12-summation (for subtraction of the contributions of carbon clusters), and (5) autocorrelation.

### 3.8.1. Classification of Organic Mass Spectra

A spectral classifier is a linear or non-linear algorithm where the values of spectral features are input and the output is a numerical response. In the best case the output estimates a structural property or indicates a compound class. A classifier output can also be used as a (complex) spectral feature. A classifier is defined by the features used and by a set of parameters. For instance a linear classifier with output  $y$  is given by

$$y = \sum [x(i) - a(i)] * b(i) \quad (5)$$

with  $a(i)$  being the scaling bias for mean centering and  $b(i)$  the loading factor for feature  $i$ . The classifier parameters are estimated from reference data and may be re-estimated when COSIMA data are available.

### 3.8.2. Comparison and Classification of Mass Spectra from Minerals

The inorganic contribution to the mass spectra exhibits the mineral constituents of the grains. Apart from established methods as laid out by Stephan (2001), we will follow up on a concept, in which the analysis is based in a first step on the average solar system isotopic ratios of the main rock forming elements (Mg, Si, S, K, Ca, Fe). Classifiers for mineral ions are ratios and ratios of ratios of intensities of atomic ions and a variety of molecular ions (each summed up over their isotopic varieties). In a next step, a more detailed analysis implying mathematical perturbation methods will then help to determine deviations in the cometary matter from the average solar system isotopic ratios. Engrand *et al.* (2005) have shown that the minerals enstatite,

olivine, serpentine, and talc can be well discriminated by applying multivariate data analysis to TOF-SIMS data.

### 3.8.3. *Detection of Cometary Grains*

Once a target has been exposed to cometary dust, and retrieved, and has been checked by COSISCOPE, a site identified is scanned by the ion beam in order to localize the area, which is different from the plain target. The test will start with a rather low mass resolution and a low lateral resolution. Depending on the results, the mass resolution is increased and the focus of the ion beam is reduced. These tests are repeated until a grain is identified or until stopped for other reasons. This search for a cometary grain is performed automatically. At the end, the grain is characterized using classifiers as described above.

### 3.8.4. *Comparison of Individual Sites*

The experience from the analysis of the Halley data suggests that cometary matter is rather similar in composition: most particles were an intimate mixture of mineral grains and an organic coating. The ratio of both components varied in the ions (!) over 8 orders of magnitude, while the variation within each component was quite small. There were, however, a few particles, the spectra of which were dominated by Fe and S ions or showed an unusual  $^{12}\text{C}/^{13}\text{C}$  ion ratio (Jessberger and Kissel, 1991). With this in mind, it is the task of site comparison to point to such sites, which seem to have an unusual composition. The actual comparison is done with the use of the classifiers described above.

### 3.8.5. *Software*

This chapter covers the software for the control of the COSIMA ground support equipment and the in-flight software onboard the COSIMA flight instrument.

## 3.9. THE GROUND SUPPORT EQUIPMENT (GSE) FOR COSIMA

The GSE consists of a Pentium-based industrial PC with a visual display unit or a laptop used as such. Inside the PC's case is a dedicated power supply used to power the instrument. The operating system of the GSE is DEBIAN LINUX.

The GSE has several modes of operation:

- direct instrument control: In this mode the GSE is connected directly to the instrument. It is equipped with an interface card acting like the spacecraft's interface. The GSE also provides the power to the instrument and emulates the spacecraft functions of telecommanding and receiving telemetry.
- instrument control via the Rosetta Spacecraft Interface Simulator (SIS): The GSE controls the spacecraft simulator which in turn emulates the spacecraft functions of telecommanding, and receiving telemetry.

- telemetry interpretation when connected to the Central Checkout System or ground data segment: the GSE passively receives the COSIMA data and uses dedicated software to interpret them. The GSE can start the COSIMA instrument residing test and forward the test result as 'COSIMA OK' or 'COSIMA NOT OK' to the Central Checkout System.

In all of the above modes, GSE-residing, dedicated software is used to interpret the COSIMA telemetry data received from the instrument directly or via a network. Housekeeping data, events, and science data are saved and can be viewed at any time. The GSE displays in near real time the instrument's state in graphical format according to the housekeeping values and events sent by the instrument. The instrument can be commanded via graphical or command-line based user-interfaces.

During flight, the GSE is used to compose and check telecommands before they are sent as request to the operations center.

#### **4. In-Flight Operation**

For a versatile instrument like COSIMA the operational concept turns out to be highly complex. Several aspects have to be accommodated:

- instrument safety
- instrument maintenance
- instrument autonomy
- efficient data generation
- efficient indium usage
- dust sample temperature history
- accommodate software revisions, especially the final version after hibernation
- on board power constraints
- on board temperature constraints
- unexpected turnoff

Since there is a unique instrument usage profile on ROSETTA, only part of the operational software was on board when COSIMA was launched. Except for short time periods of maintenance, the instrument is 'OFF' from 2004 through 2012. Maintenance operation is needed to stimulate the liquid indium ion emitter, to avoid the formation of a crust, which would hinder the flow of the metal, and also for the motors in the Target Manipulator Unit, in order for the moving parts to stay lubricated. Later, around 2014, it is 'ON' sporadically for dust collection and initial test runs. For the last 6 months (or 4400 hours) of the mission, when dust will be most abundant, it should be running almost continuously. During this time period, all of the instruments would want to be turned on, and consequently the spacecraft would become too hot. Therefore time, or better, power constraints have to be expected. The signal round trip time of about 1/2 hour requires the instrument to run with a large degree of autonomy.

#### 4.1. THE CONCEPT

The COSIMA operational concept is based on a maximum of independence of its subunits from one another and on the pre-definition of individual tasks and rules, upon which the on board system can schedule its activities. Of course, spacecraft orders and ground commands always have higher priority. When after launch the instrument is turned on, it will first of all conduct a self-test during which it checks all of its components, which have an interface to the microprocessor system, as well as all independent subsystems, TMU, COSISCOPE, and PIBS. After this autonomous test has been completed, which takes a few minutes, it will wait for another 5 minutes for instructions either stored on board the spacecraft or received directly from ground. Once this waiting period is expired, the instrument will resume from the activity list stored on board (should there be none, it will continue to wait). In doing so, it relies heavily on lookup tables or formulas to configure the functional elements into their operational modes, mostly into the measuring mode for positive or negative secondary ions. While the indium reservoir of the ion emitter is heated up, all of the high voltage converters have to be fed with their actual values, and the values for the deflection plates have to be set, and the timing of the primary ion source, i.e., for chopper and the three bunchers, has to be established. In a quick check, using  $H^+$  or  $H^-$  ions, the pulse width of the primary ion beam is measured and adjusted if needed. The next step is to optimize the ion transmission by scanning the primary and secondary deflection plate voltages. Finally, the mass resolution is checked (using, e.g., Ag related ions) and adjusted if needed, before nominal operation is started. In another scenario, a target unit may have to be exposed or be retrieved after exposure. In yet another mode, a series of COSISCOPE images may have to be taken, the locations of collected dust particles have to be calculated and be transmitted to the main processor system. All these activities would require a huge amount of telecommands, all of them to be issued and controlled by ground operations. Many of these commands have therefore been combined into functional groups, which can be called upon at the appropriate times.

#### 4.2. THE COMMAND STRUCTURE

For the proper operation of COSIMA, three levels of commands are implemented:

1. The *low level* commands, which write directly to the hardware cards controlling the instrument. Examples of the low level commands are: ‘sub-unit power on’, ‘sub-unit power off’, ‘set one specific voltage’, etc. The low level commands are primarily meant to be used during development and testing of the instrument. However, they can be used during the mission for detailed control of the instrument if needed.
2. The *middle-level* commands are useful combinations of several of the low level commands. Examples are: ‘move target # to dust collection’, ‘setup PIBS

operation', etc. These commands can be used during the mission to simplify 'manual' type operation.

3. The *high-level* commands combine several *middle-level* commands. They instruct the instrument what analysis program it shall perform, but hides the actual implementation level which is handled by lower level commands. Examples of the high level commands are: 'search a target for features', 'clean feature #', 'analyze feature #', etc. This is the nominal case for instrument operation during the mission.
4. Tasks are sequences of *high-level* commands, loaded into COSIMA via software commands. 128 tasks are available.

It is intended to sequence several types of such analyses of different features, as the results need assessment and decision on ground on how to proceed with the treatment of individual features. From data taken from laboratory tests during the development phase, the instrument can calculate the power profile for certain operations. Through specific commands, it can be instructed to schedule operations to stay within a given power level, if needed. Using this information, the instrument can operate autonomously for several days.

Command execution available at a specific moment is determined by the state of the instrument. High voltages, e.g., cannot be 'ON' while the target manipulator is in the process of moving targets. Each operational mode and sub-mode of the instrument has its own subset of *high-level*, *middle-level*, and of *low-level* commands which can be executed during that mode.

#### 4.3. POST LAUNCH – PRE ARRIVAL ACTIVITIES

The use of microprocessor systems in space instrumentation allows much more sophistication and optimization. Part of this in turn requires a very detailed knowledge of the properties of the hardware actually flying and of the general type of such an instrument. On the other hand, it leaves many chances to modify the operational software according to new results in the laboratory or from the actual space instrument. Used properly, this is a very powerful tool for the success of an investigation. In the case of ROSETTA, where there is a long time between delivery of the instrument to the project and the actual measuring phase, there is an important opportunity to update COSIMA's operational software. This includes only the science related part and not the sections, which control the communications between the spacecraft and the instrument.

##### 4.3.1. *Maintenance and In-Flight Operation During Commissioning*

Among the subsystems of COSIMA, there are two that need special attention and care between launch and arrival at the comet: The liquid indium ion emitters and the target manipulator. While for the emitter it is the contamination of the metal surface and a consequent deterioration of the flux properties of the metal, it is the

lubrication of the moving parts, which has to be assured in the target manipulator. Fortunately, action for both can be accommodated in a small routine, which is run every 9–13 months, starting with the initial in-orbit checkout of COSIMA. The following actions will be started:

- heat the indium reservoir of emitter 1
- move motor 1 for a number of steps
- move motor 2 for a number of steps
- make emitter 1 emit for up to 10 minutes
- cool emitter 1
- heat the indium reservoir of emitter 2
- move motor 3 for a number of steps
- move motor 4 for a number of steps
- make emitter 2 emit for up to 10 minutes
- cool emitter 2

As the increasing experience suggests, refined versions of these actions can and will be implemented in the instrument's operational software, and the duration and the power consumption will be documented.

Rosetta commissioning was carried out in 2004, the COSIMA instrument was operated in-flight after nearly a decade of development and tests on the ground. Positive and negative SIMS ion mass spectra were taken of one of the Ag metal targets, the resulting spectra are shown in Figure 18a and b, respectively. The inorganic and organic ions and molecules show up in separable and well resolved mass peaks, such as Si and C<sub>2</sub>H<sub>4</sub> or Fe and C<sub>4</sub>H<sub>8</sub>. Small amounts of organic molecules being known to be present in cometary dust such as CN are adsorbed on the blank metal target and reveal themselves in the SIMS mass spectra. Since COSIMA carries also a heating station for the target, the level of volatile contamination can be further decreased before exposure of the target to the cometary dust. Comparison with mass spectra taken of the same target in 2002 before launch already shows a slight decrease of volatiles such as hydrocarbons absorbed on the target surface after residing only about 6 months in space. This contamination by organic molecules was, in part, released from the insulation material of the electrical harness and from boxes used for ground transportation. Note that the Ag peaks are caused by ions released from the target and the In peak is due to primary ions from the ion source. For high secondary ion rates, the mass spectra show saturation effects due to dead-times inherent in the ion detector counting electronics, best visible adjacent to each of the intense Ag isotope peaks.

#### 4.3.2. *The Ground Laboratory Program*

During the cruise phase to the comet as well as while the probe is actually analyzing cometary dust; an active laboratory program will be maintained. While the SIMS method is routinely applied for relevant geological and planetological studies, the TOF-SIMS technique will benefit from this terrestrial work with the COSIMA RM

reference model. Additionally, growing experimental and methodological expertise comes from the day-to-day work with relevant samples at the TOF-SIMS laboratory instrument currently in use at the University of Münster. The complex mixture of organic and inorganic material, expected to make up the comet, will result in equally

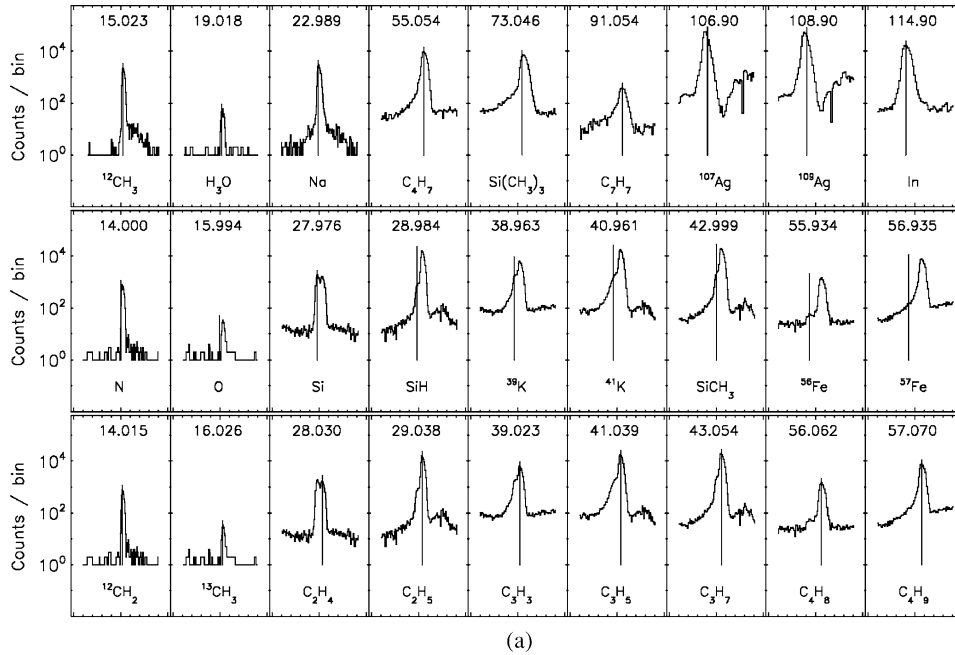


*Figure 18.* (a) First COSIMA in-flight positive secondary ion mass spectrum (SIMS). Each window is centered on examples of mass peaks of the COSIMA time-of-flight mass spectra. The mass range is  $\pm 0.5$  amu and the number of secondary ions is given in counts/mass bin. The potential identification of atoms or molecules and their mass are labeled in each window, the position of the mass is indicated by a vertical line. For the same integer mass number, organic molecule peaks are located to some extent to the right, while the inorganic ion peak is located to the left of the integer mass number. The top panel refers to mass peaks with a unique atom or molecule identification. The center panel refers to mass peaks with potentially both organic and inorganic atoms or molecules within the same mass range of  $\pm 0.5$  amu. Inorganic elements or molecules containing inorganic elements are labeled in each window. The bottom panel refers to the organic molecules, mainly hydrocarbons, identified in the ion spectrum. Comparison of the center and bottom panel reveals the mass resolution of the COSIMA instrument, sufficient to resolve e.g. Si and  $C_2H_4$  (b) First COSIMA in-flight negative secondary ion mass spectrum (SIMS). Each window is centered on examples of mass peaks of the COSIMA time-of-flight mass spectra. The mass range is  $\pm 0.5$  amu and the number of secondary ions is measured in counts/mass bin. The potential identification of atoms or molecules and their mass are labeled in each window, the position of the mass is indicated by a vertical line. For the same integer mass number, organic molecule peaks are located to some extent to the right, while the inorganic ions peak is located to the left of the integer mass number. Electronegative elements such as O, F or Cl and I clearly show up in the negative ion spectrum. The negative ion spectrum also shows electrons sputtered off the grids within the reflectron. The electron peaks are shifted by a defined time lag from the main ion peak.

*(Continued on next page)*

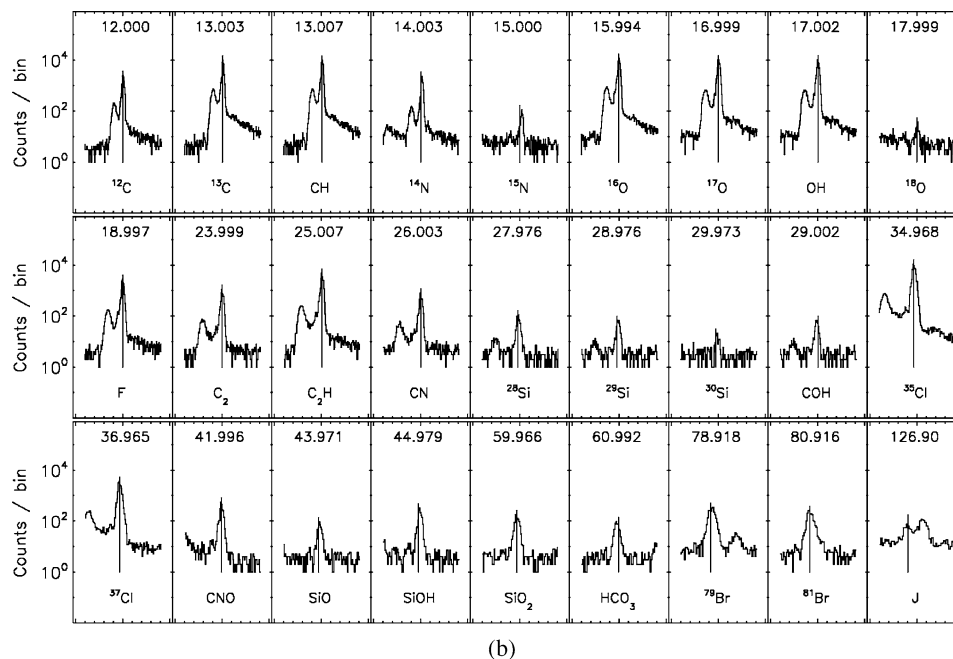


Figure 18. (Continued)

complex mass spectra. They have to be disentangled to provide information on the chemical, isotopic, and molecular composition of the particles that reflect the origin, history, and present state of cometary matter. The particle-to-particle variation will testify to its diversity, i.e., to the extent of the pristine nature of these materials, and to its stellar sources. Interpreting the mass spectra requires calibration. Calibration here is not meant to mimic the experiment in a one-to-one scale in the laboratory, but rather to understand the processes, which control ion formation with complex samples, as well as the instrumental parameters of mass separation and ion detection. To that end, state-of-the-art laboratory TOF-SIMS analyses with utmost lateral and mass resolution of various materials available on Earth will be performed, which include, but are not limited to:

- Interplanetary dust particles (IDPs). Some of these small and difficult-to-analyze particles actually may stem from comets. It is an active research topic to sort these out and distinguish them from asteroidal IDPs. IDPs of a certain class are mixtures of inorganic and organic matter and as such represent the best analog material for the COSIMA case.
- Carbonaceous chondrites: They are mechanical mixtures of fine-grained low-temperature matrix and carbon-rich phases (kerogen) with high-temperature clasts, single minerals, and chondrules. Their overall chemical composition is solar as far as the condensable elements are concerned. They most closely represent

and witness the Early Solar System materials and processes. They are regarded as the base line material in planetology.

- Certain IDPs and chondrites contain particles with non-standard isotopic composition of a number of elements that point towards their nucleosynthetic stellar sources. These particles (stardust or presolar particles) will serve to learn how to obtain the relevant information from cometary matter.

The extraterrestrial materials mentioned above are not as pristine as we expect cometary dust to be. IDPs are altered to an unknown extent during passage through the atmosphere, deceleration processes and residence in the stratosphere; carbonaceous chondrites were subject to metamorphism and aqueous alteration on their parent bodies. Consequently, for the analysis of organic (and icy) components anticipated in cometary particles artificial analogs are needed. They are siliceous vaporization deposits contaminated with organic substances. Certainly not all possible organic substances can be analyzed, but rather we will perform TOF-SIMS measurements of relevant substance classes.

As mentioned above, these analyses are performed with the highest possible mass and (where appropriate) lateral resolution. In addition, the temporal evolution of the mass spectra is evaluated by using the data from all primary ion pulses. This will give hints to a possible layering within the material and/or validate influences, which the TOF-SIMS method may cause in the material (by, e.g., ‘radiation damage’). New statistical and chemometric methods and procedures, now under test, will be further developed and applied.

The laboratory program will benefit from and be adjusted to new insights, which will come from the analysis of the samples returned by Stardust in 2006.

## 5. Anticipated Results

### 5.1. THE MINERAL PHASE

The anticipated results of the investigation of the mineral phase of the cometary dust are manifold:

- First, we shall establish the mean composition of the main elements, and then check whether this varies from grain to grain, either within the statistical variance or beyond that. In the latter case we’ll be able to identify various classes of minerals.
- Second, the distribution of molecular ions should be sensitive to the order structure of the minerals, may they be in an amorphous or in one of several crystalline states. This would give an important clue to the thermal and radiation history of the dust.
- Third, once an elemental and molecular distribution of the main isotopic contribution is established, the contribution of the minor isotopes can be measured

from grain to grain, needed for the question whether various stellar sources have played a role to form the dust.

- Fourth (last but not least), a cross-correlation of the types of organics sitting upon the same grain will give insight into aspects of the real grain forming process as well as to possible catalytic interferences between each phase. This is important for the ‘Origin of Life’ topic and its relation to nano-systems.

## 5.2. THE ORGANIC PHASE

The refractory organic phase will most probably be an intimate mixture of a lot of individual species. But still, the history of grain formation and the incorporation of them into cometary nuclei is reflected – at least partially – in the distribution of the organic species. Substance class analysis will provide clues to whether the organic phase is mainly produced by condensation of vapors and subsequent radiation processing with polycondensation and oligomerization, etc., or, if it is mainly produced by condensation of larger molecules and aggregation of small refractory particles.

Another important question is, whether the organic material in comets is suitable to start the onset of life on earth. In this case, the analysis will show that the precursors of such molecules needed for life’s self-organization by exothermal reactions with liquid water are present.

As water usually shows up in different ways in the mass-spectra, clues to the source of water in the comet may be found, too: is it just a condensation of water ice in the grains, or, is it the result of long-term radiation induced processes, such as polycondensation or Born-Haber-type processes, or is perhaps a fraction of the water in a comet produced by thermally induced reactions, when the comet approaches the sun?

COSIMA results thus address the main questions concerning the origin of the hydrosphere, and further on, the biosphere on earth.

## 6. Conclusions

Writing up this paper was an opportunity to review the general concept of COSIMA. It seems that the hardware is very well suited to perform the measurements on cometary dust. As mentioned earlier, at the time of writing, the software was still in a rudimentary state awaiting all the model specific values and the definition of individual tasks. Since no instrument hardware was available at this time, those inputs still had to wait. In this sense, the description is somewhat incomplete, since it is the software that ultimately defines the ‘personality’ of an instrument. Fortunately, progress on the subsystem level was good enough to assure that the overall performance of COSIMA will meet the scientific objectives. COSIMA’s

hardware is very well suited to perform in-situ measurements on cometary dust (in almost a decade from now). The flight software will be adapted to the experience gained with the COSIMA laboratory model, and the onboard data analysis will be updated according to the results from cometary analog material. SIMS is a very sensitive analysis method, not only for the bulk composition, but also for the surface layers of the collected cometary dust. Unlike previous measurements with impact dust mass spectrometers, COSIMA is capable to analyze the composition as a function of the stratification within the dust grains and layers of ultrafine dust or even attogram dust grains, provided that the cometary flux of these particles is sufficient. Therefore, COSIMA constitutes the next generation dust analysis instrumentation and will provide valuable insight into the cometary dust building blocks, restraining models of comet history, morphology, organic and inorganic chemistry, mineralogy, and petrology. The data from COSIMA and its operation will be the reward for the many fights against technical and bureaucratic problems.

### Acknowledgements

One of us (J. K.) wants to mention that COSIMA would not have happened without the continuous support of G. Haerendel, director at the Max-Planck-Institut für extraterrestrische Physik in Garching, B. Feuerbacher, director of the Institut für Raumsimulation of the DLR, the funding agencies DARA and later DLR (grant number 50 QP 9711 3) with G. Hartmann, E. Lorenz, W. Kempe, and M. Otterbein, and last not least, H. von Hoerner, director of the contractor vH&S GmbH, who also serves as Co-PI and has conceived ever cheaper ways to build COSIMA. Substantial hardware and software contributions, without which COSIMA could not work, were contributed by COSIMA Co-Is from France, Finland, and Austria.

### References

- Dahl, D. A.: 1997, INEEL, Idaho Falls, Idaho 83415, DHL@inel.gov: The SIMION software manual (and later versions).
- Engrand, C., Kissel, J., Krueger, F. R., Martin, P., Silén, J., Thirkell, L., et al.: *Rapid Commun. Mass Spectrom.* **20**, 1361.
- Jessberger, E. K., and Kissel, J.: 1991, In: R. Newburn, M. Neugebauer, and J. Rahe (eds.), *Comets in the Post-Halley Era*, Springer Verlag, Heidelberg, pp. 1075–1092.
- Kissel, J., Sagdeev, R. Z., Bertaux, J. L., Angarov, V. N., Audouze, J., Blamont, J. E., et al.: 1986, *NATURE* **321**(6067), 280.
- Kissel, J., Brownlee, D. E., Büchler, K., Clark, B. C., Fechtig, H., Grün, E., et al.: 1986, *NATURE (Encounters with Comet Halley – The First Results)* **321**(6067), 336.
- Kissel, J., and Krueger, F. R.: 1987, *NATURE* **326**, 755.
- Krueger, F. R.: A Feasibility Study for CoMA, part 1, Aug. 1988, part 2, Jan. 1989, and part 3, Sept. 1989.
- Krueger, F. R., Korth, A., and Kissel, J.: 1991, *Space Sci. Rev.* **56**, 167.

COSIMA – HIGH RESOLUTION TIME-OF-FLIGHT SECONDARY ION MASS SPECTROMETER

- Mamyrin, B. A., Karatyev, V. I., Shmikk, D. V., and Zagulin, V. A.: 1973, *Zh Eksp. i Teor. Fiz.* **64**, 82 or: *Sov. Phys. JETP* **37**(1), July 1973.
- Mazets, E. P., Sagdeev, R. Z., Aptekar, R. L., Golenetskii, S. V., Guryan, Yu. A., Dyachkov, A. V., et al.: 1987, *Astronomy Astrophys.* **187**, 699.
- McDonnell, J. A. M., Green, S. F., Grün, E., Kissel, J., Nappo, S., Pankiewicz, G. S., et al.: 1989, *Adv. Space Res.* **9**(3), 277.
- Schwab, M.: 1998, CEMEC GmbH, Obererlbach, FRG: Design of the COSIMA Target Manipulator, (private communication), 1998.
- Stephan, T.: 2001, *Planet. Space Sci.* **49**, 859.
- Varmuza, K., Werther, W., Krueger, F. R., Kissel, J., and Schmid, E. R.: 1999, *Int. J. Mass Spectrom.* **189**, 79.
- Varmuza, K., Kissel, J., Krueger, F. R., and Schmid, E. R.: 2001, In E. Gelpi (Ed.), *Advances in Mass Spectrometry*, vol. 15 (Wiley & Sons, Chichester), p. 229–246.
- Werther, W., Demuth, W., Krueger, F. R., Kissel, J., Schmid, E. R., and Varmuza, K.: 2002, *J. Chemom.* **16**, 99.
- Zscheeg, H., Kissel, J., Natour, Gh., and Vollmer, E.: 1992, *Astrophs. Space Sci.* **195**, 447.